To the Graduate Council:

I am submitting herewith a thesis written by John J. Tomlinson entitled "Performance Evaluation of a Solar-augmented Heat Pump with Offpeak Heating." I recommend that it be accepted in partial fulfillment of the requirements for the degree of Master of Science, with a major in Mechanical Engineering.

Robert L Reid

Robert L. Reid, Major Professor

We have read this thesis
and recommend its acceptance:

Gary V Smith

J F Sucec

James A. Dahl

Accepted for the Council:

L Evans Reed

Vice Chancellor
Graduate Studies and Research

X

PERFORMANCE EVALUATION OF A SOLAR-AUGMENTED HEAT PUMP WITH OFFPEAK HEATING

A Thesis

Presented for the

Master of Science

Degree

The University of Tennessee, Knoxville

John J. Tomlinson

August 1980

3044894

ACKNOWLEDGMENT

In a project of this size, much of the work could not have been done without the help of others. I want first to recognize the Tennessee Valley Authority who provided funding for this study and, hopefully, will find the results useful. I also want to thank Al Bedinger and Bernie McGraw of the Energy, Environmnet and Resources Center for the project's inception, initial experimental design, and continued monitoring for the duration of the data collection period. Don Miller of the Instrumentation and Controls Division at Oak Ridge National Laboratory provided technical expertise and built much of the instrumentation used in data collection. In addition, Dr. Robert L. Reid, Professor of Mechanical Engineering at the University of Tennessee and my major professor provided valuable suggestions throughout the experiment. Finally, I would like to thank my wife, Joan, not only for her help in preparing this thesis but also for her encouragement, patience and support during my graduate studies.



ABSTRACT

An experimental residential building located in Knoxville, Tennessee was provided with air solar collectors, rock bed storage, offpeak electric heating and a back-up heat pump. The solar system operated in parallel with the air-to-air heat pump and solar modes of operation had priority over the heat pump and all resistance heating. To minimize the purchase of onpeak electricity, the control strategy provided space heating during all onpeak hours with the operation of a 1/2 hp air blower alone.

The facility was instrumented to determine electrical usage of individual system components, and system heat flows using air-side heat flow measurements. Experimental results for the period November 5, 1979 through April 13, 1980 indicate an offpeak fraction of 0.83 and a seasonal system performance coefficient of 1.66. These results indicate that the system would be beneficial to a winter-peaking electrical utility and could also operate economically under time-of-day rates.

TABLE OF CONTENTS

CHAPTER		PAGE
I.	INTRODUCTION.	1
	Offpeak Heating	1
	The Heat Pump	4
	Combined Solar-Heat Pump Systems.	7
	Experimental Objective.	10
II.	SOLAR-AUGMENTED HEAT PUMP SYSTEM.	11
	System Description.	11
	Modes of System Operation	20
III.	SOLAR-AUGMENTED HEAT PUMP SYSTEM INSTRUMENTATION.	26
	Instrumentation Description	26
	Air-side Heat Flow Measurements	34
	Data Acquisition.	37
IV.	SYSTEM PERFORMANCE.	44
	Component Performance	44
	Data System Performance	47
V.	EXPERIMENTAL RESULTS.	49
	Data Analysis	49
	Results	55
	Conclusions	68
	Recommendations	69
LIST OF REFERENCES.		72
APPENDICES.		75
APPENDIX A.	FACILITY COMPONENT DESCRIPTION	76
APPENDIX B.	BUILDING HEAT LOAD CALCULATION	77

APPENDIX C. OFFPEAK CONTROL THERMOSTAT SETTINGS. . . 80

APPENDIX D. EXPERIMENTAL ERROR ANALYSIS. 82

APPENDIX E. DATA ANALYSIS COMPUTER PROGRAM 84

VITA. 93

LIST OF FIGURES

FIGURE		PAGE
1.	TVA Peak Load Day.	3
2.	The Heat Pump.	6
3.	Combined Solar-Heat Pump Systems	8
4.	Solar-augmented Heat Pump Facility	11
5.	Solar-augmented System	13
6.	The Offpeak Loop	17
7.	The Offpeak Controls	18
8.	System in Solar Collection Modes	21
9.	System in Storage-to-Space Mode.	23
10.	System in Heat Pump and Offpeak Modes.	24
11.	System Instrumentation	28
12.	Storage Resistance Temperature Device.	29
13.	Rock Storage with RTD Sensors.	31
14.	RTD for Heat Flow Measurement.	31
15.	Turbine Flowmeter.	32
16.	Heat Flow Measurement Logic.	40
17.	Offpeak Control Modification	48
18.	System Heat Flows.	52
19.	The Building Heat Load	59
20.	Collector Performance on February 4.	61
21.	Time-of-Day Rate Comparisons	67

CHAPTER I

INTRODUCTION

Offpeak Heating

The rapid depletion of our fossil fuel and other nonrenewable energy resources is an issue of great concern and makes the efficient use of these resources imperative. As these energy resources become more scarce and more difficult to obtain, they become more expensive for the utility, and as a result, for the consumer.

The costs of electrical power generation fall into three categories as follows:

1. Customer-related costs, which are incurred by the utility regardless of the amount of energy consumed by a customer. Typical customer-related costs are metering, meter reading and accounting costs.

2. Energy-related costs, which vary according to the quantity of kilowatt-hours used during a period.

3. Demand-related costs, which are generally associated with generating facilities required to meet the maximum rate of consumption of electrical power.

In the TVA region, the largest of these costs are energy-related, the second largest are demand-related and a relatively small portion are customer-related (1). Energy-related costs can be stabilized or perhaps even

---

Numbers in parentheses () refer to references.

reduced by substituting renewable energy sources for those nonrenewable sources which are now used for electric power generation. Demand-related costs can be reduced only through utility load leveling whereby low cost base-load electrical generating capacity such as coal or nuclear are substituted for the more expensive and more flexible power generation by peak and intermediate load plants and fuels. Load leveling may be encouraged on the customer side of the meter by the utility's instituting time-of-day pricing. This would make electricity purchased during onpeak times more expensive thus reflecting the additional demand-related cost to the utility, and that purchased during offpeak times, less expensive. Time-of-day pricing makes the possibility of storing low cost base-load utility energy attractive. The fact that storage heating systems are cost effective in service areas supplied by winter peaking utilities is well established (2), and currently a number of electric utilities are testing and evaluating electric storage heating systems (3).

Due primarily to the residential space heating load in the Tennessee valley, the utilities served by the TVA are winter peaking. Figure 1 shows the components of the TVA annual peak system load (1,p.29). This annual peak was estimated to be 22,584 megawatts occurring on January 11, with the coincident residential component amounting to 48 percent. Since the largest single contributor to the system annual and daily utility peak is the residential

TVA SYSTEM WINTER PEAK DAY

JANUARY 11 ,1978

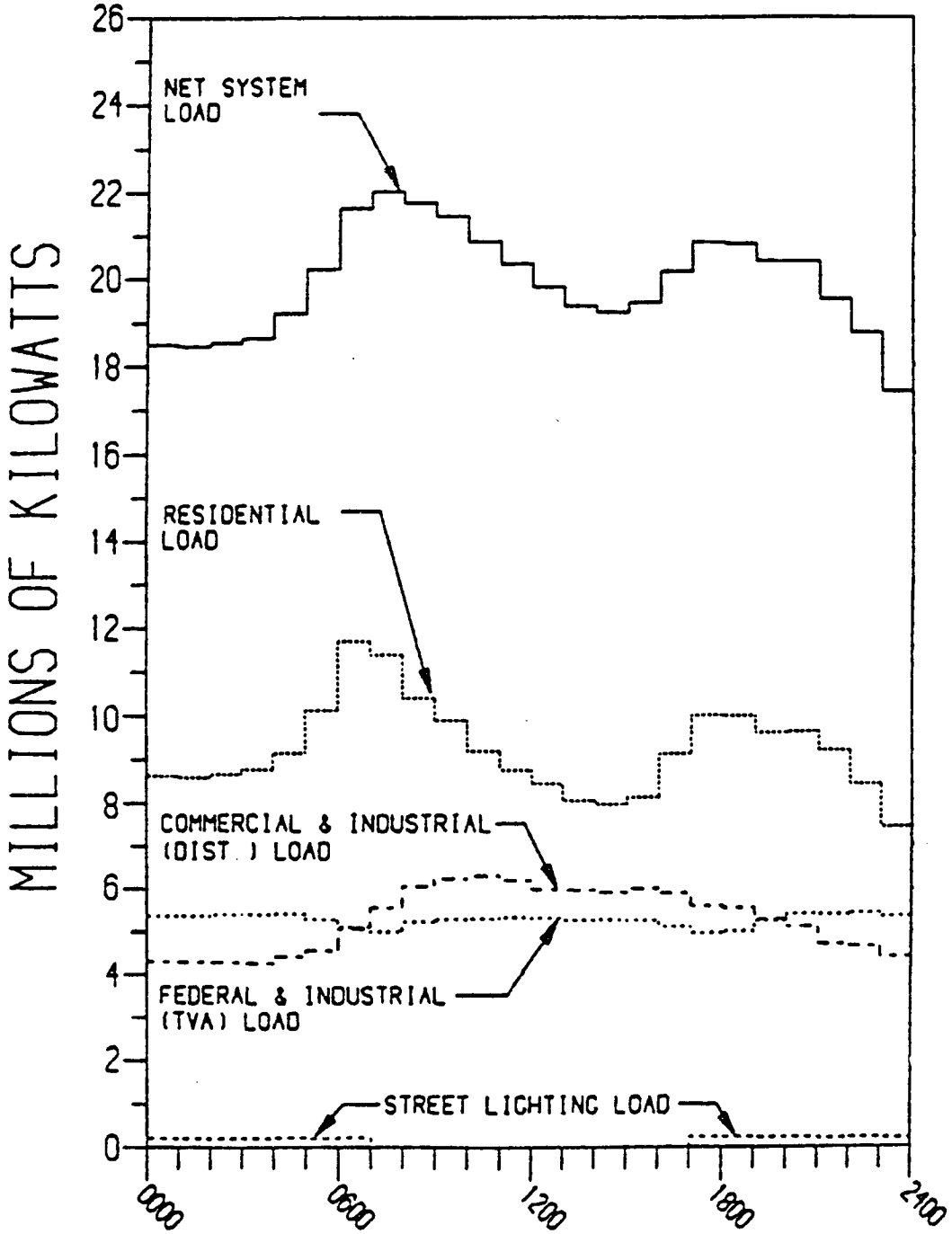


FIGURE I. TVA PEAK LOAD DAY.

customer, aims to alleviate the peaking problem with its associated high costs must be directed toward the residential sector. However, a time-of-day rate study by the TVA (4) showed that simply providing time-of-day electricity pricing did not guarantee permanent alteration of onpeak consumption. The second year of this two-year study found electrical usage patterns of the participants returning to pre-study levels, thus suggesting a lessening of attention given to the time-of-day pricing by the participants. These results indicate that automatically controlled residential heat storage is needed to guarantee constant offpeak usage patterns continuously. Simulation studies (5,6) and actual demonstrations (7) of residential space heating systems consisting of offpeak storage heating components have revealed substantial reductions in onpeak electrical usage.

The Heat Pump

The conventional residential heat pump is a compression-refrigeration system which transfers heat from a cooler fluid to a warmer fluid. The impossibility for this transfer to take place spontaneously without the addition of work forms the basis for Clausius' statement of the second law of thermodynamics. Using the work to transfer rather than generate thermal energy as in the case of electrical resistance heating, provides the heat pump with a more efficient and economical method of space heating.

A measure of heat pump efficiency is a dimensionless quantity called the coefficient of performance (COP) and is generally greater than one. The COP for a heat pump in the heating mode is defined as the ratio of (a), the heat supplied to the load to, (b) the work input to the heat pump. A typical COP would be three meaning that for every BTU of electrical energy needed to drive the heat pump compressor and fans, three BTUs are delivered to the interior of the house. The "missing" two BTUs were removed from the outside air and pumped into the house, thus the integrity of the first law of thermodynamics is maintained. If the heat pump is an air-to-air type as shown in Figure 2, the evaporator coil is outside the house and removes heat, QL, from the air so that the refrigerant changes from a low pressure mixture of liquid and vapor to a low pressure saturated vapor. The compressor increases the pressure of the refrigerant changing its thermodynamic state into the superheat region in, ideally, an isentropic process. The superheat vapor then enters the condenser and heat, QH, is rejected into the conditioned space. Exiting the condenser as a saturated liquid at high pressure, the refrigerant then flows through the expansion valve, thereby reducing the pressure and returning the fluid to the evaporator to complete the cycle. Although Figure 2 depicts typical heat pump components, the COP of an ideal heat pump with Carnot efficiency can be stated by Equation (1-1).

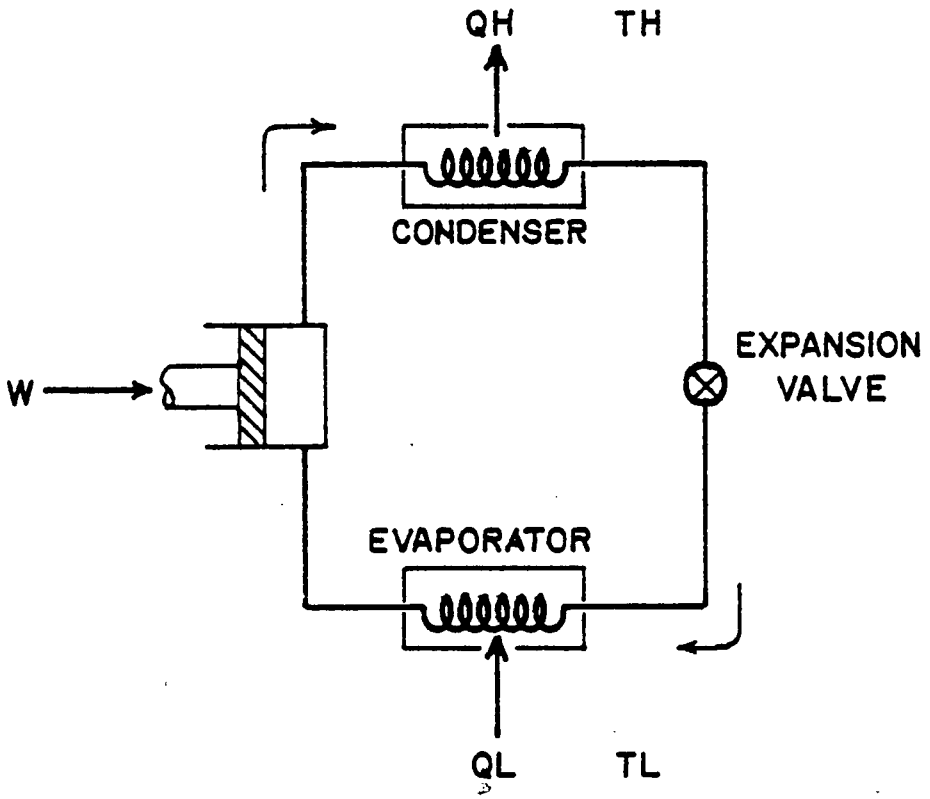


Figure 2. The Heat Pump.

$$COP_{IDEAL} = \frac{1}{1 - \frac{T_L}{T_H}} \qquad (1\text{-}1)$$

The heat pump performance is strongly affected by the ratio of the two temperatures, TL, the evaporating temperature and TH, the condensing temperature. Equation 1-1 indicates that as TL decreases the heat pump COP decreases resulting in an undesirable feature of the heat pump: the ability of a heat pump to deliver heat to a house decreases with decreasing outside temperatures, contrary to the house heating demand, which rises with progressively colder

outside temperatures. Periodically frost which builds up on the evaporator coils prevents effective heat transfer and must be removed through the heat pump defrost cycle thus increasing operating costs and requiring additional controls.

Combined Solar-Heat Pump Systems

The coupling of a heat pump to a solar collection system is promising, and may be done in three basic ways as shown in Figure 3.

In the series system the solar storage is used as the source for the heat pump. This is done by allowing the evaporator coils of the heat pump to absorb thermal energy directly from storage when the storage temperature is too low to heat the house directly. This combination of collector, storage and heat pump is often termed a solar-assisted heat pump and provides the following advantages:

1. Since the solar collectors can supply the thermal energy at a higher temperature than outside air, then even on days where direct solar heating would not be possible, the COP of a solar assisted heat pump would be greater than that for a heat pump alone.

2. Since the solar collector temperatures could be lower, collector losses would decrease.

3. Because solar collection temperatures can be lower than would otherwise be necessary, less efficient (and consequently less expensive) collectors may be used.

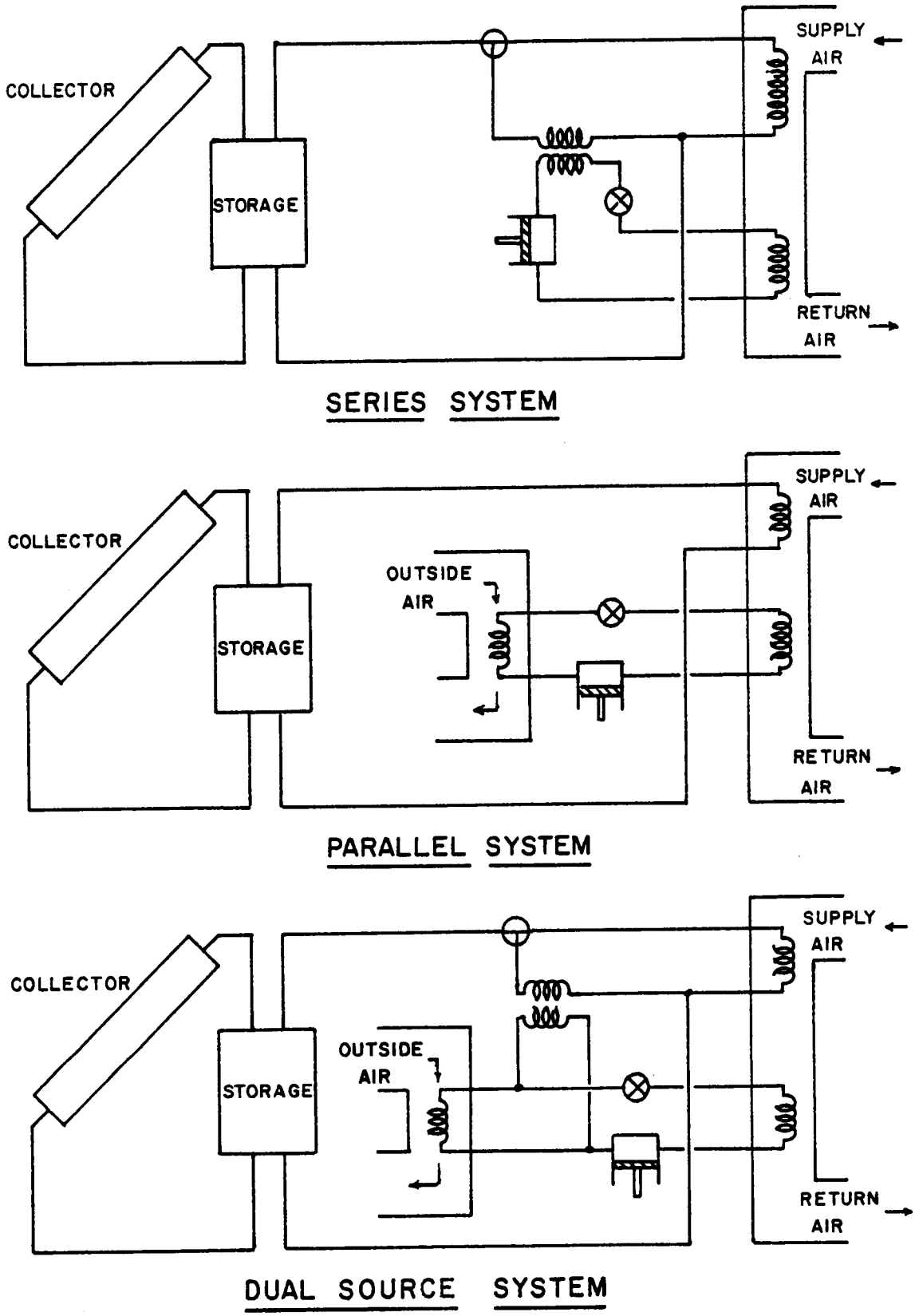


Figure 3. Combined Solar-Heat Pump Systems.

The parallel system simply uses the heat pump as an auxiliary energy source, and other than using the same return air heating duct as the solar system, operates in the conventional way, removing thermal energy from the outside air and transferring it to the inside of the house. The parallel system has advantages listed as follows:

1. Since the solar system operates independently from the heat pump, retrofitting a residence with an existing heat pump would be straightforward.

2. The parallel system is the simplest of the solar-heat pump combinations.

By having two evaporators, one in the ambient air and one in the storage loop, the dual source system has the option of using either heat source depending on the one that results in the higher system COP. In this way, the dual source system takes advantage of the best performance characteristics of both the series and parallel systems.

In spite of the higher COP delivered by both the series and dual source solar-heat pump combinations, Freeman et al. (8) showed that over the heating season, the thermal performance of the parallel system is superior to that of both the series and dual source systems. Morehouse and Hughes (9) confirmed the superiority in thermal performance of a parallel over a series combination. A resolution of this paradoxical conclusion lies principally in the average storage temperature for each of the three systems. In the dual source and series

systems, storage temperatures are rarely high enough for the house to be heated directly so that not only is purchased energy required to transfer solar energy into storage, but also to operate the heat pump virtually whenever space heating is required. Frequently in the parallel system, the COP is much higher since fan work is the only purchased energy input during periods of direct solar heating.

Experimental Objective

In view of the utility peak load problem which can be mitigated by use of automatically controlled thermal storage, and reductions in purchased energy requirements demonstrated by the heat pump and active solar systems, it was decided to provide a residential building with a parallel solar heat pump system, herein referred to as a solar-augmented heat pump, with auxiliary offpeak heating. To minimize the impact on the daily electrical utility peak demand, it was resolved to design the building heating system so that the space heating requirements could be met during all onpeak hours each day by a single air handler unit.

CHAPTER II

SOLAR-AUGMENTED HEAT PUMP SYSTEM

System Description

The building which was modified for this test is a small uninsulated slab on grade garage of floor area 720 square feet and volume 9000 cubic feet, located near Knoxville, Tennessee at 35.5 degrees North latitude and 83.6 degrees West longitude. A photograph of this facility can be seen in Figure 4, showing the solar collector array mounted on the roof. This collector array consists of twelve air collectors ducted in parallel so that each collector is connected to the same supply air plenum. The

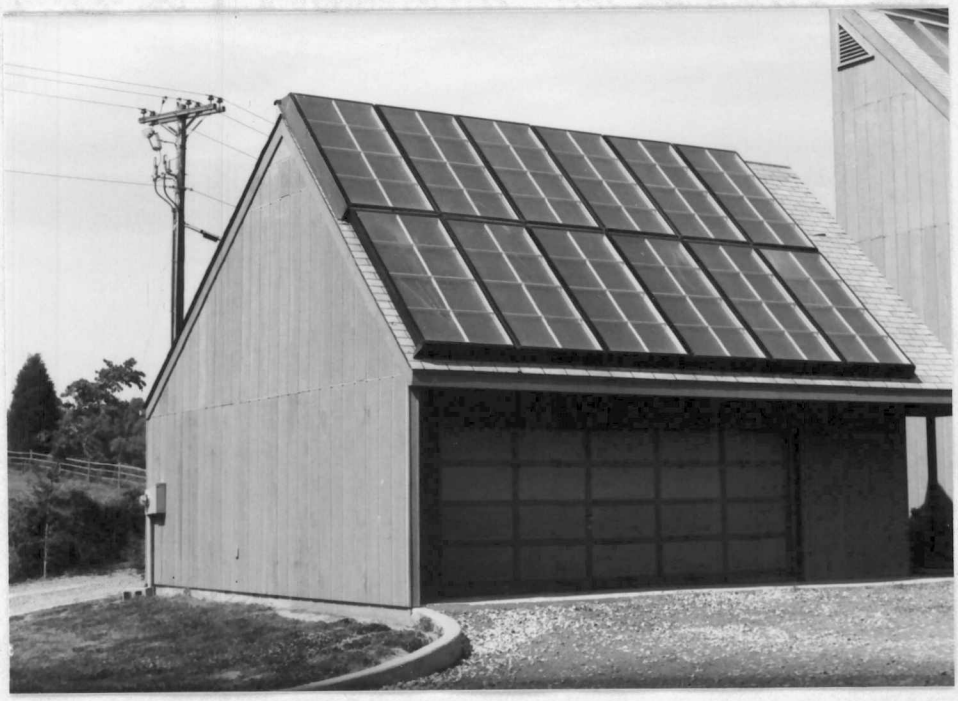


Figure 4. Solar-augmented Heat Pump Facility.

net aperture area of each collector is 26.4 square feet giving the array itself a composite area of 316.8 square feet. An outer collector cover of tedlar fiberglass and an inner cover of Filon provide a total cover transmissivity of 83%. The absorber is a sandwich of two sheets of aluminum with an air plenum between them. The absorber surface is painted with a selective coating having an absorptivity of 0.95 and emissivity of 0.90. The collector array has an advertised maximum efficiency of 0.57 at an air flow rate of 900 cubic feet per minute. The collector array was mounted directly on the pitched roof at a tilt angle of 45 degrees and azimuthal angle of 10 degrees west of south.

Figure 5 shows schematically the interior of the facility with the individual system components and the connecting air ducting. The storage unit located inside the conditioned space is an insulated box made using conventional stud wall construction and contains a 28-gage sheet metal liner. The unit is 7 feet long, 7 feet wide and 6.5 feet tall and contains 260 cubic feet of limestone rocks. This rock has a density of 100 pounds per cubic foot and a specific heat capacity of 0.22 BTU per pound mass per F. The storage size was not based on the accepted ratio (10) of collector area to storage volume, but rather on the building heat demand during a six-hour onpeak period. Since this demand must be satisfied entirely by thermal energy from storage, the storage volume

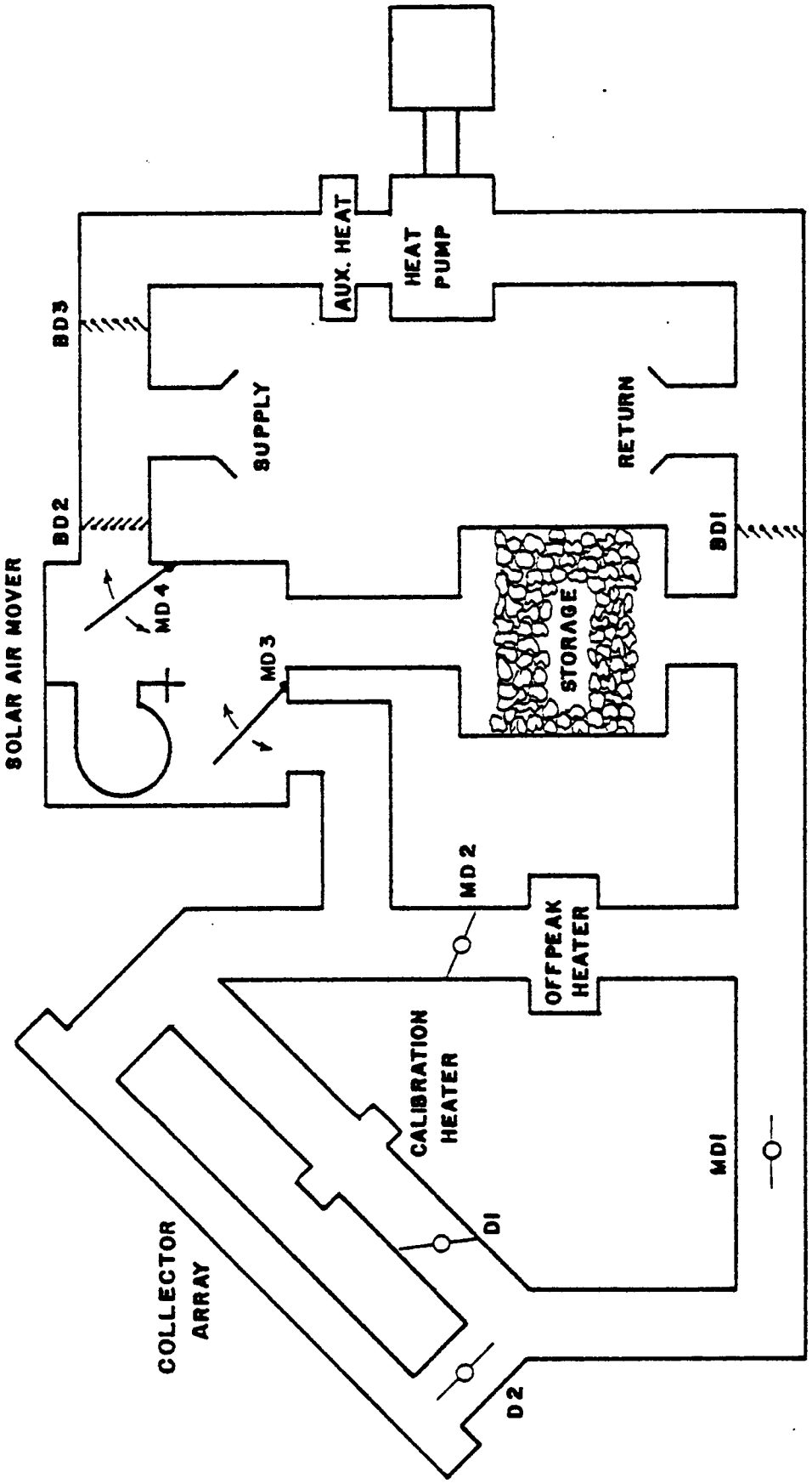


FIGURE 5. SOLAR-AUGMENTED SYSTEM.

is approximately 60 percent greater than would otherwise be necessary.

The solar air handler is a self-contained unit housed in a 2 feet x 3 feet x 3 feet sheet metal housing which is provided with three openings; a 19 inch x 12 inch inlet from the collector array, a 19 inch x 12 inch inlet/outlet to storage, and a 19 inch x 15 inch outlet to the conditioned space. Two motor-driven dampers, MD3 and MD4, a blower with a 0.5 horsepower electric motor and a controller provide the solar air mover with the capability of supplying air from the collector array to storage or to the conditioned space, or from storage to the conditioned space. The selection of the proper damper positions for these air delivery modes is made by the controller and three sensors, one located in the collector array outlet, one at the top of storage, and the other at the bottom of storage. The controller is programmed so that the solar air mover is inactive unless the collector temperature is 45°F greater than the cold (bottom) storage temperature, at which point collection starts. When the difference between the collector temperature and cold storage temperature drops to 25° F collection will stop. The controller is wired for a delivery temperature to space of 85°F. This means that the controller will not indicate that heat is available from storage unless the hot sensor in the top of storage indicates a temperature greater than or equal to 85°F.

The auxiliary heat back up is a conventional air-to-air heat pump. The outdoor unit consisting mainly of a compressor and evaporator coils has a nominal heating capacity of 31,500 BTU/hr. at an outside temperature of 47°F and 19,500 BTU/hr. at 17°F. The indoor unit consists of an air handling unit, condenser coils and an auxiliary 20 KW electric resistance heater which provides supplemental heating with the heat pump when needed as well as supplying heat to the building during the heat pump defrost cycle.

The indoor thermostat used to control the operation of the solar components and the heat pump consists of three heating stages. The first stage bulb in the thermostat directs the collected solar energy so as to satisfy the space heating requirement. If the solar heat is not sufficient to maintain the space temperature, the second stage bulb engages, activating the heat pump compressor and indoor air handling unit. Should the indoor temperature continue to fall, a third stage bulb in the thermostat engages the auxiliary resistance heater in the heat pump. In this way, the use of collected solar energy for space heating has priority over the heat pump and auxiliary heater which require larger amounts of purchased energy.

Offpeak heating requires components in addition to those mentioned for a solar-augmented heating system. The offpeak heater loop, also shown in Figure 5, provides thermal energy to the rock storage via the solar air mover

during offpeak hours whenever sufficient insolation is unavailable. The offpeak resistance heater has a 5 KW and a 10 KW element positioned in a short section of 18 inch x 18 inch insulated ducting. Relays in the heater assembly allow a choice between 5 KW, 10 KW and 15 KW rates of energy input. During times when the offpeak heater is not used, motorized damper, MD2, is closed to prevent the air flow from passing through the offpeak leg. When the offpeak heater is being used, MD2 is opened and MD1 closed to isolate the collector loop. The motorized damper MD2, the heater itself and the associated offpeak ducting are shown in Figure 6 and indicate the relatively small increase in system size by incorporation of an offpeak heating loop in a residential heating system with existing storage.

Efficient offpeak heater controls require input from several system parameters. Firstly, a timer is used to allow the offpeak heaters to turn on only during designated offpeak hours. Secondly, two thermostats which have sensing bulbs placed at different levels in the storage bin indicate the degree to which storage is initially charged at the beginning of an offpeak period, and finally, a third thermostat bulb placed outside of the building is used to indicate to what level storage should be charged to meet the space heating demand during the subsequent peak period. The control system designed to meet these objectives is



Figure 6. The Offpeak Loop.

presented in Figure 7, showing the offpeak duct containing the motorized dampers MD1 and MD2 along with the two stage duct heater. The operation of the offpeak control system is initiated at terminals 15 and 24 which are located on the solar air mover. When the solar air mover is delivering solar energy either to space or to storage, 24 VAC exists between these terminals, thereby opening MD1. At the same time relay R1 opens which inhibits the offpeak heaters. If the solar air mover is not delivering collected solar energy, zero VAC exists between terminals 15 and 24, and the offpeak sequence is initiated. Motorized damper MD1 shuts, isolating the collector loop and, simultaneously, relay R1 closes. If the timer indicates that an offpeak period is in effect, and the

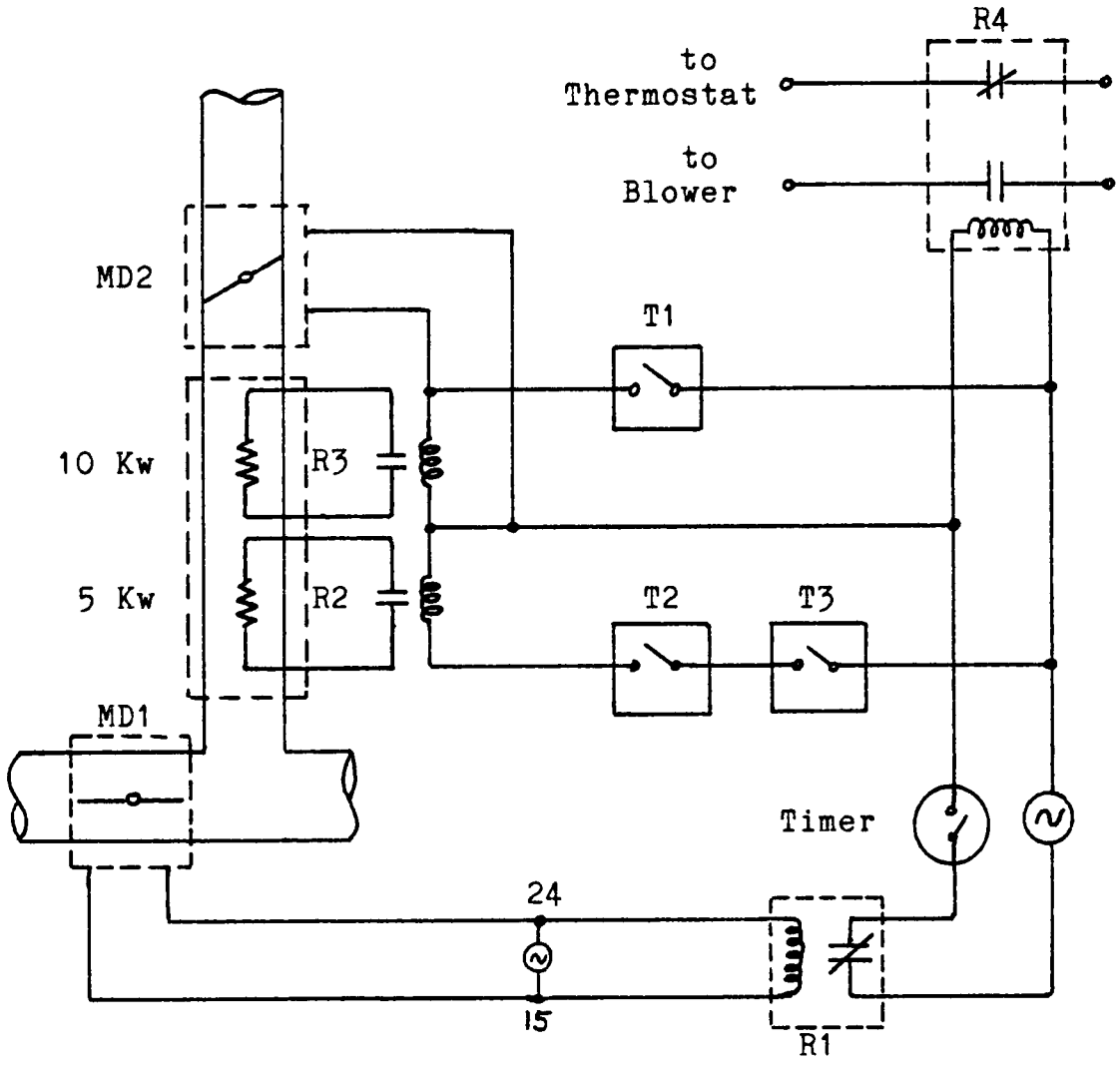


Figure 7. The Offpeak Controls.

upper storage thermostat T1 is not satisfied, then 24 VAC is presented to motorized damper MD2, and relays R3 and R4. Motorized damper MD2 opens allowing air to flow through the offpeak leg, and R3 closes thereby activating the 10 KW heater. At the same time, R4, a double pole relay, turns on the blower in the air mover and "opens" a connection from the room thermostat to the solar air mover. This "open" circuit prevents a 24-volt control signal from the thermostat from reaching the solar air mover when first stage heat is indicated. In this way MD4 (see Figure 5) continues to direct heated air to storage rather than to space. It is only when the space temperature continues to drop that the second stage of the thermostat is engaged which turns on the heat pump. If during an offpeak period the outside air temperature is quite low and the temperature in the bottom of storage is low, thermostats T2 and T3 are not satisfied and close to activate relay R2 which provides an additional 5 KW to the air stream in the offpeak loop. Appendix C describes the method used to determine the initial settings for thermostats T1, T2, and T3.

To simulate the interior loads which would occur in an inhabited house, a heater along with four fluorescent fixtures provide a total of 24 Kw-hr. of energy to space each day. The daily schedule of the interior load simulator follows a programmed sequence.

Time (EST)	Energy (Kwh)
0000 - 0700	3.5
0700 - 0900	3.0
0900 - 1700	8.0
1700 - 2200	7.5
2200 - 2400	2.0

Modes of System Operation

To minimize purchased energy requirements for space heating, the solar-augmented system was designed and operated giving solar energy priority. The system is shown in Figure 8 operating in the two collection modes, collected solar energy to storage and to space. In these modes of operation as well as in all other normal modes, manual damper D2 is open and D1 closed as shown, to force all air moving in the collector loop to pass through the collector array. The purpose of the calibration heater leg of the system will be described later. If the space heating demand is satisfied, heated air exits the collector array, is drawn through the solar air mover and with MD4 in the vertical position, passes into storage. The now cooled air leaves the bottom storage plenum and returns to the collector array. This air is prevented from passing into the conditioned space by backdraft damper DB1. The solar-to-storage mode continues until (a) the temperature difference between collector exit and storage inlet falls to the pre-programmed 25°F and the solar air mover turns

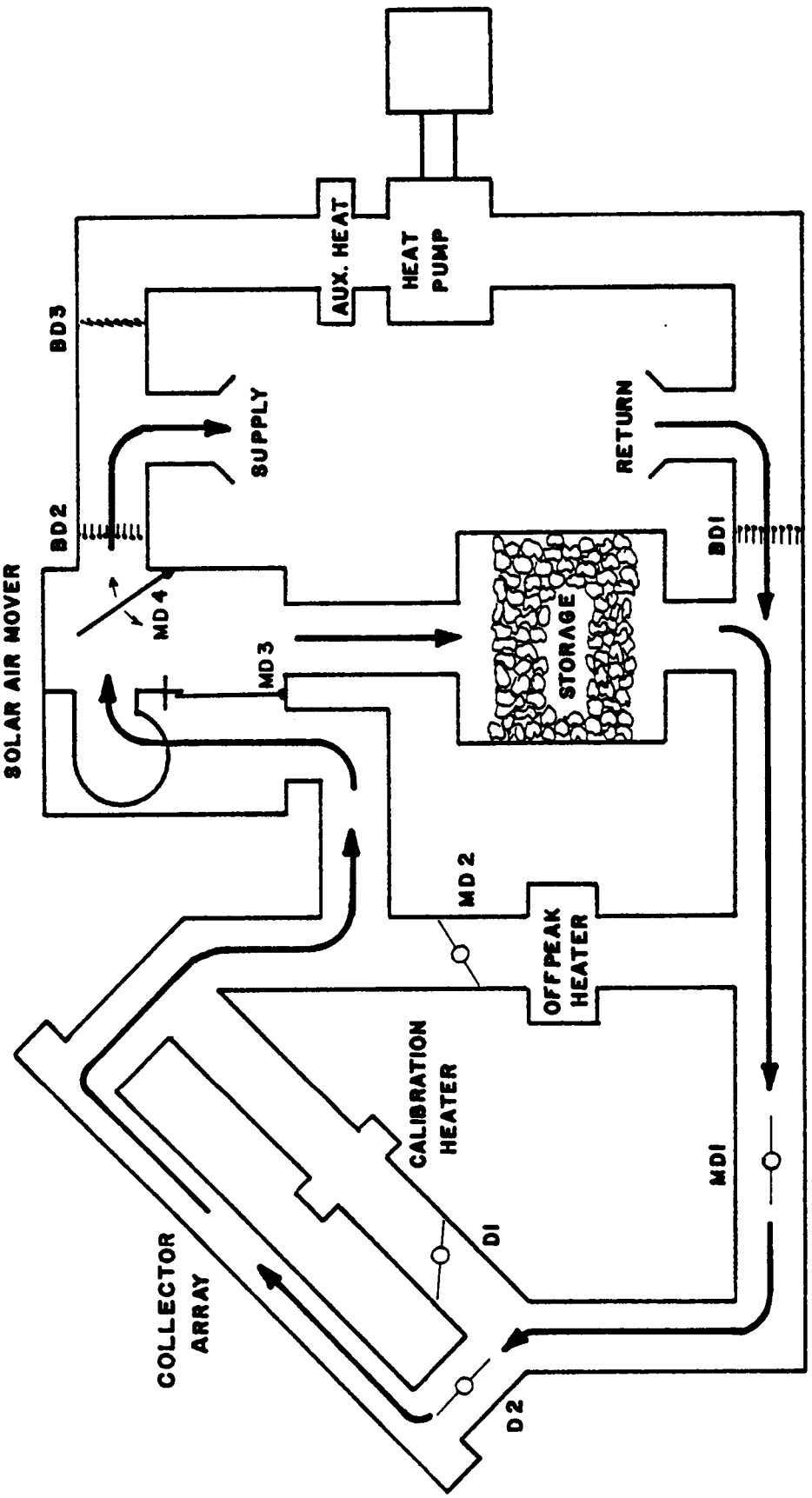


FIGURE 8. SYSTEM IN SOLAR COLLECTION MODES.

off, or (b) the space temperature drops enough to engage the first stage heating bulb of the indoor thermostat. In the second case, motorized damper MD4 simply falls to the horizontal position thereby sending the heated air into space. In this solar-to-space mode, backdraft damper DB3 ensures that air leaving the solar air mover arrives in the heated space through the supply duct rather than passing through the heat pump loop.

The system operates in the storage-to-space mode when (a) sufficient solar energy is unavailable, and (b) the top storage plenum temperature is at least 85°F, and (c) space heating is required as indicated by the first stage of the indoor thermostat. Operation of the dampers MD3 and MD4 in this second priority mode, shown in Figure 9, causes heated air to exit the top of storage and pass through the solar air mover and into space. The return air passes through dackdraft damper DB1 and into the bottom of storage. In the storage-to-space mode, motorized damper MD3 effectively inhibits the return air from entering the collector and offpeak loops.

In the event that heat from storage or heat directly from the collector array is unable to meet the space heating demand and the space temperature continues to drop, the second stage bulb of the thermostat is engaged. The second stage bulb (a) turns on the heat pump, (b) places damper MD4 in the vertical position, and (c) turns off the solar air mover blower. Figure 10 shows this mode of heat

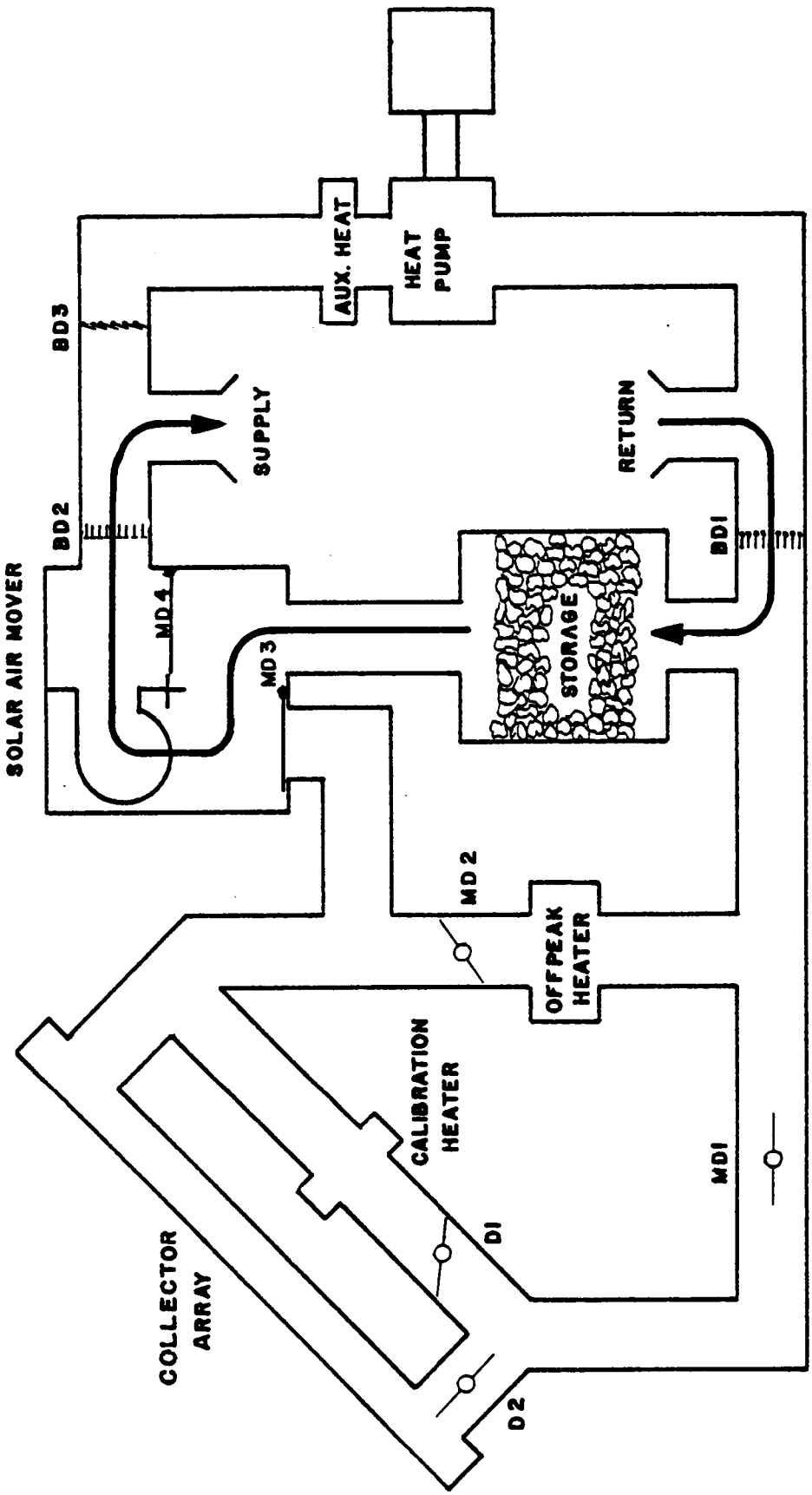


FIGURE 9. SYSTEM IN STORAGE-TO-SPACE MODE.

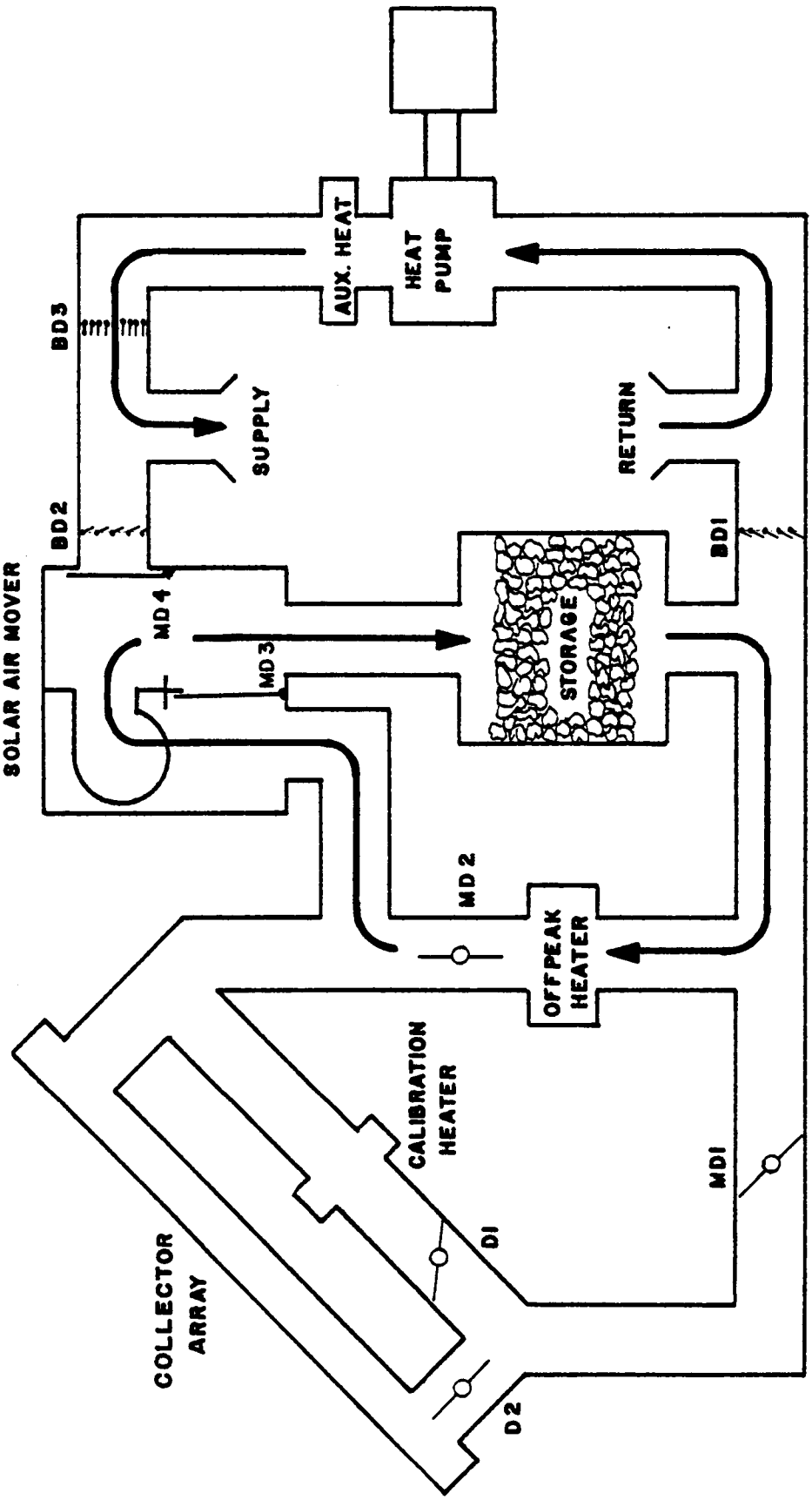


FIGURE 10. SYSTEM IN HEAT PUMP AND OFFPEAK MODES.

pump operation and direction of the associated air flow to space. A third stage bulb in the wall thermostat regulates the operation of additional auxiliary resistance heaters in the heat pump loop. These heaters assist the heat pump and help maintain the comfort level of the thermostat setting.

The offpeak heating mode also shown in Figure 10 may not necessarily be in effect while the heat pump is operating. During the offpeak periods when storage is not fully charged, the offpeak controls simultaneously close motorized damper MD1 and open damper MD2. This allows the solar air mover to recirculate the heated air through storage. The offpeak mode is terminated by the offpeak controls as previously discussed when either the control thermostat T1, T2 and T3 are satisfied or when the offpeak period designated by the timer ends.

CHAPTER III

SOLAR-AUGMENTED HEAT PUMP SYSTEM INSTRUMENTATION

Instrumentation Description

The selection of instrumentation for this experimentation was dictated by several factors such as sensor reliability, and linearity over the operating range, and ease of adaptability through electronic interfaces to a completely automatic data acquisition system.

Insolation was measured by a standard Eppley black and white pyranometer. The light sensitive area of this pyranometer consists of a disk divided into alternating black and white sectors. The hot junctions of a differential thermopile are thermally connected to the black sectors and the cold junctions connected to the white. A potentiometric output from this thermopile indicates the difference in sector temperatures which, in turn is a measure of the insolation. This pyranometer was mounted on a building approximately 30 yards south of the test facility and 25 feet above ground and was tilted 45° from the vertical. Both tilt and azimuth angles were the same of that of the collector array so that the sky view factor of both collector and pyranometer were the same. The pyranometer was calibrated against a secondary standard before installation and, to date, has received annual inspections and adjustments as needed. An error analysis

of a pyranometer which receives global radiation is difficult to assess, however taking all of the various factors into account, Latimer (11) indicates that an instrument error of 3.6% exists for the Eppley black and white. Insolation values were integrated electronically to produce hourly totals of accumulated solar energy.

The locations of instruments used to measure temperatures and duct air flows in the facility are shown in Figure 11. The temperatures T4-T10 at seven regular levels in the rock storage were measured using platinum resistance thermometry. These RTD's or resistance temperature devices are nominally 3 feet long with the transducer itself located near the tip of each, as seen in Figure 12. By inserting these RTD's in copper thermowells placed in storage before filling with rock, the RTD's could easily be removed and replaced if necessary. The length of this type of RTD was ideal allowing temperature stratification along the central vertical axis of storage to be measured.

Errors in the potential difference produced by this sensor can arise from two sources (a) instrument inaccuracies and (b) supply current instabilities. The constant current circuits which were used in this experiment were designed and constructed at the Oak Ridge National Laboratory (ORNL) and continuously provide 1.0000 $\pm$ .0001 milliamperes to all RTD's. Such a small error renders inaccuracies due to part (b) above, negligible.

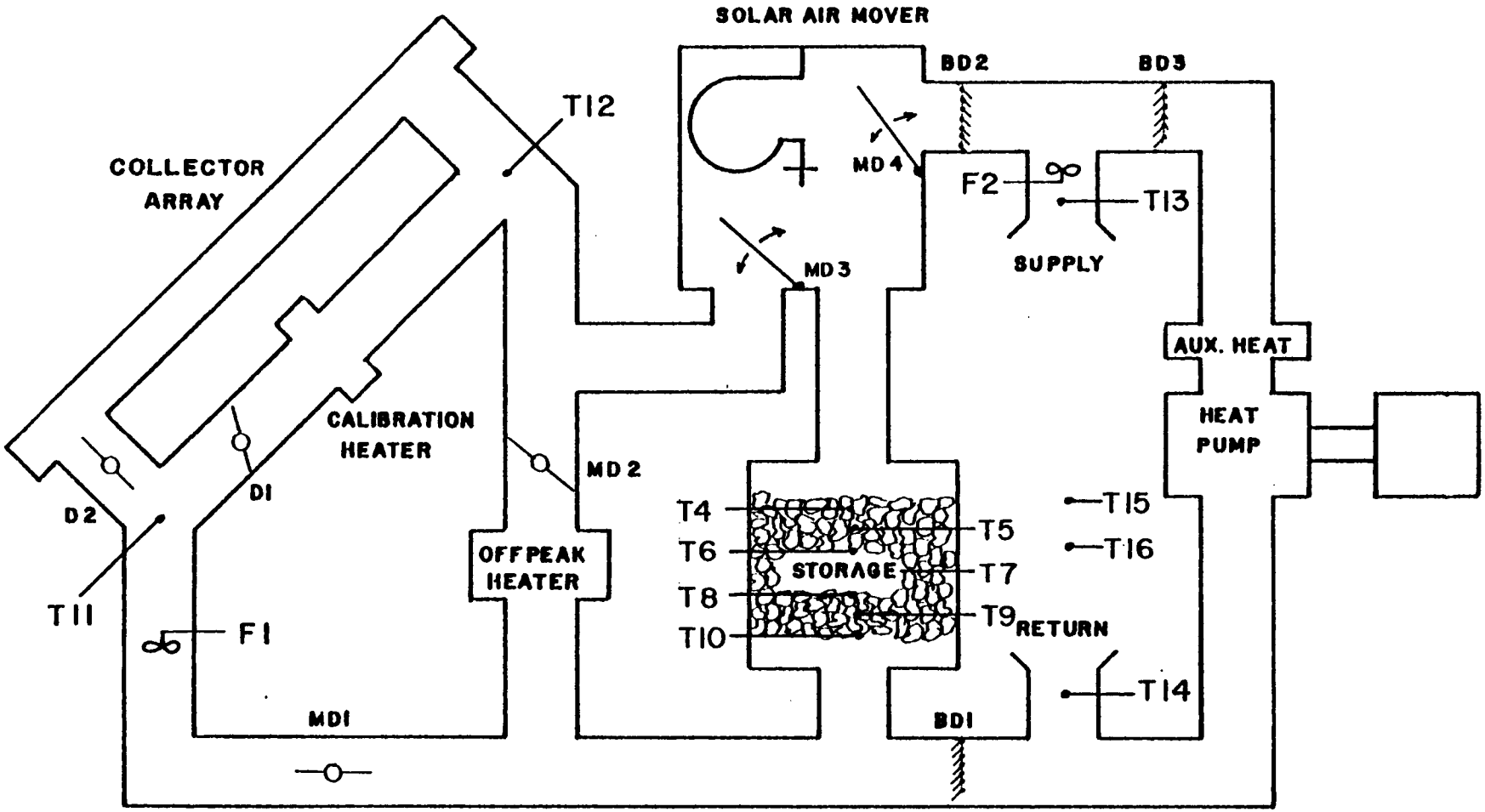


FIGURE 11. SYSTEM INSTRUMENTATION.

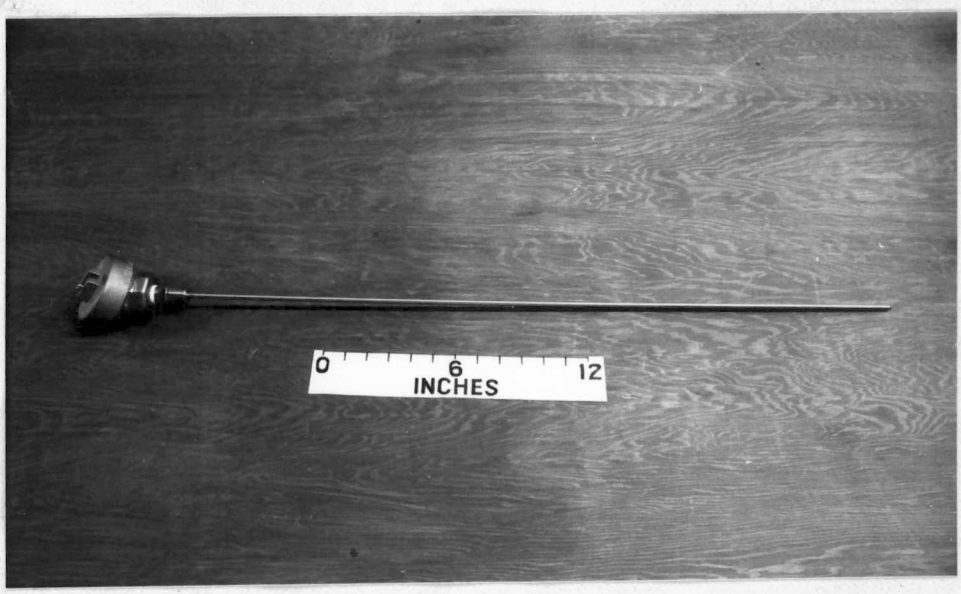


Figure 12. Storage Resistance Temperature Device.

However tests (12) of the combined performance of these RTD's and current supplies indicated an instrument error of 0.3% at 90°C, easily within the range necessary to accurately determine rock storage temperature stratification. Figure 13 shows the seven RTD's T4-T10 in place in the storage wall and the connecting wiring.

Figure 11 shows four more RTD's, T11, T12, T13 and T14 which were located in the ducting. These RTD's form the basis for the two air heat flow measurements described later in this report. Each of these RTD's is 25 feet long and is wound on a light sheet metal frame in such a way as to assure uniform sampling of the temperature of the air moving through the frame. These RTD's on metal frames shown in Figure 14 were placed in the ducting and obvious air leaks were plugged with silicone sealant. In immersion tests at ORNL with these RTD's, it was found that the 25-foot RTD's exhibit an instrument error of 2.5% when supplied by the same type of constant-current as actually used in the facility instrumentation.

The second type of instrument used as a component for air heat flow measurements were small turbine flowmeters, F1 and F2, with capacitive readout shown in Figure 15. These flowmeters were chosen for their sensitivity and small resistance that they caused to the moving air stream in the ducts. In this way, the air stream velocity was monitored with little additional system pressure drop due to the presence of sensors. The turbine rotor in these

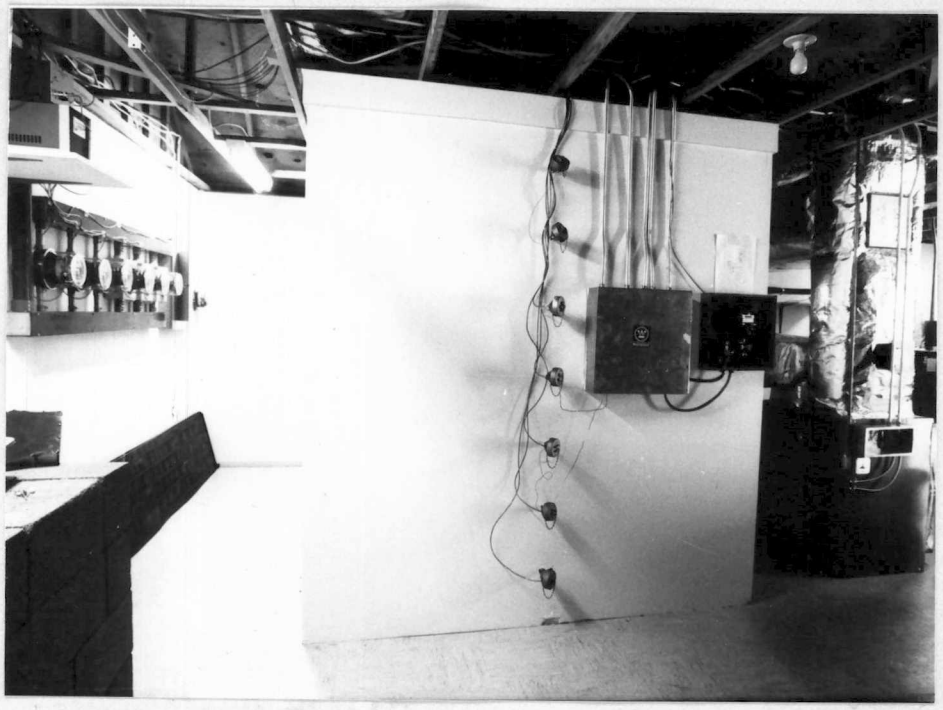


Figure 13. Rock Storage with RTD Sensors.

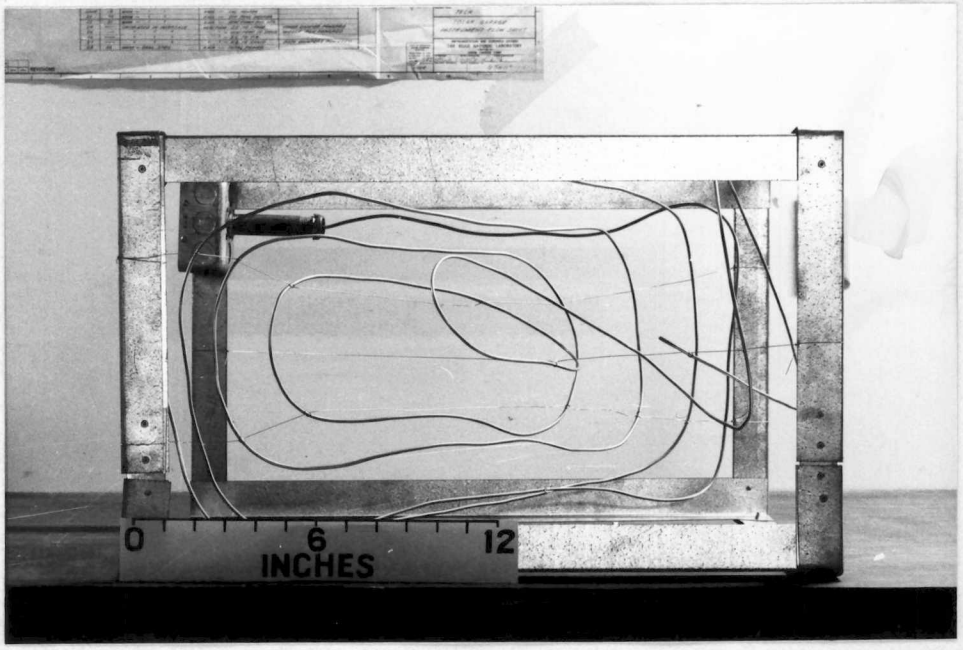


Figure 14. RTD for Heat Flow Measurement.

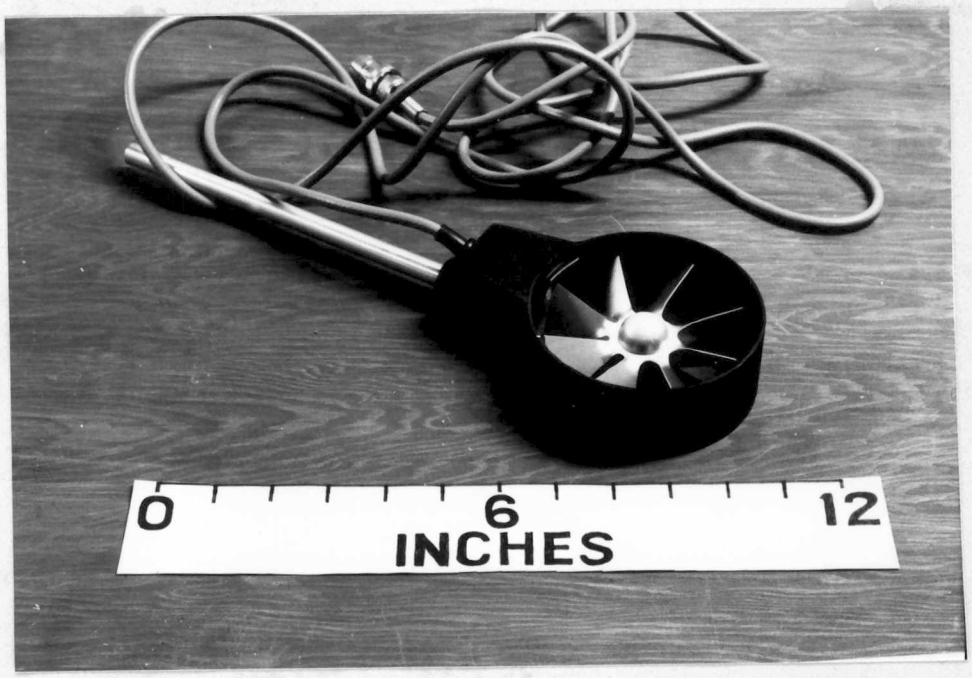


Figure 15. Turbine Flowmeter.

flowmeters spins in jeweled bearings and assures reliability over the duration of the experiment. Although no published data existed on the precision of flow measurements by this flowmeter, communications with the manufacturer indicate (14) that flow measurements in their laboratory are typically replicated to within 3%. This was used as the accepted value for the analysis in this experiment.

To measure individually the electrical energy consumptions of the various system components, watt-hour submetering was used. In this way the purchased energy used for any period by (a) the heat pump indoor unit, (b) the heat pump outdoor unit, (c) the heat pump auxiliary strip heaters, (d) the solar air mover, (e) the calibration heater, (f) the offpeak heater and (g) the total building could be monitored separately. The watt-hour meters used were standard single-phase General Electric meters differing only in their K_h ratings to accomodate the demands of the system components. The Knoxville Utility Board which supplied the meters for the experiment, initially certified (15) that each meter was accurate to within 0.5%.

Space wet and dry bulb temperatures were measured using temperature probes. These are high impedance solid state stainless steel probes about the size of a pencil which were supplied with a nominal 5 VDC to give a current output directly proportional to probe temperature. The

current output was dropped through a precision resistor to give a potential difference proportional to the space temperature. In compliance with the manufacturer's data, space temperatures were measured to an accuracy of $\pm$ 1.0°C at 25°C. This pair of sensors was located approximately 6 feet above the floor near the room thermostat. The wet bulb consisted of a small moist sock covering one of the probes and was aspirated by a fan 2 minutes before any data were taken.

Air-side Heat Flow Measurements

Two heat flow stations are shown in Figure 11, page 28. The collector heat flow station consists of RTD's T11 and T12 and flowmeter F1. The space heat flow station consists of T13, T14 and F2. The operation of these stations and assumptions made require an explanation.

Sensible heat addition to or removal from a moving air stream in residential ducting can be stated by Equation (3-1) as follows:

$$\dot{Q} = \dot{m} C_p \Delta T \qquad (3\text{-}1)$$

Where $\dot{Q}$ is the rate of heat removal or addition to the moving air stream, $\dot{m}$ is the mass rate of flow of the air, C_p is the specific heat of the air at constant pressure, and ΔT is the change in air temperature between the inlet

and outlet. Equation (3-1) may be rewritten for a nonuniform air velocity distribution in a duct in the following way:

$$\dot{Q} = C_p\left[\int_{\text{DUCT AREA}} \rho \vec{V}\cdot\hat{n}\,dA\right]\Delta T = \rho C_p \bar{V} A \Delta T. \qquad (3\text{-}2)$$

In Equation (3-2), ρ is the mass density of the air, A is the cross sectional duct area, and $\bar{V}$ is the mean air speed. While in this experiment, $\bar{V}$ was not directly measured, the constant speed blowers used provided invarant velocity profiles in the ducting such that the relationship

$$\bar{V} = K(FO) \qquad (3\text{-}3)$$

exists, where K is a constant, and FO is the flowmeter output signal. Even though FO is proportional to $\bar{V}$, determination of $\bar{V}$ is not possible since K is unknown. Substitution of Equation (3-3) into Equation (3-2) yields

$$\dot{Q} = (\rho C_p K A)(FO)(\Delta T). \qquad (3\text{-}4)$$

To determine the heat flow by measuring FO and ΔT does not

necessarily mean that the individual quantities ρ, C_p, K, and A be known, but only their product. This product may be found through the following calibration procedure. In Figure 11, page 28, manual damper D2 is closed and D1 opened. With the system in the collector to storage mode and the solar air mover blower on, the calibration heater is turned on. In this way a measured rate of energy, $\dot{Q}_{CAL}$, is passed through the collector heat flow station, resulting in a temperature change of $(\Delta T)_{CAL}$ and flowmeter output of $(FO)_{CAL}$. Substitution of these quantities into Equation (3-4) yields the expression for the unknown product,

$$\rho C_p KA = \left[\frac{\dot{Q}}{(FO)(\Delta T)} \right]_{CAL} . \qquad (3\text{-}5)$$

The return air to the collector heat flow station for the duration of the experiment remained between 65°F and 80°F. Since the flowmeter was placed in this return air, the values of ρC_p were constant to within 3% of the nominal value (16), a fact which was included in the error analysis of Appendix C. Once the value of $\rho C_p KA$ was obtained in the calibration procedure using Equation (3-5), the system was returned to normal operation by turning off the calibration heater, opening damper D2 and closing D1. Collected solar energy could now be determined using Equation (3-4) because a value or calibration constant for the product ($\rho C_p KA$) was known.

Once determined, the calibration constant was placed in the memory of the data acquisition system to be mulitplied by the accumulated product of (FO) and (ΔT). The calibration constant was then used to quantify the heat flow from the collector array to space, and collector array to storage. Unmeasured duct losses in these two modes are considered later in this report.

The space heat flow measurement calibration took place in much the same way. The system was placed in the heat pump to space mode, with only the indoor unit blower and auxiliary heaters on (the compressor was off for the calibration). Since the auxiliary heater as well as the blower supply heat to the moving air, the "calibration heater" in this case consisted of the heat contribution from both. A calibration constant for this heat flow station was determined using T13, T14 and F2 and measured energy from the heat pump watt-hour meters. This constant placed into memory of the data acquisition system served in a similiar way to measure space heat flows. Thus heat flows into space, whether from the heat pump or storage could be measured.

Data Acquisition

During the experiment, the output from each sensor was modulated electronically to produce either analog or digital signals for the automatic data acquisition system. System temperatures measured by RTD's T4 - T10 and space

temperatures T15 and T16 presented analog signals (a potential difference) to the data acquisition system. Since these were linear signals, having stored in memory each sensor's characteristics in terms of slope (millivolts/°C) and intercept (millivolts at 0°C), the sensor temperature could be quickly computed by the data acquisition system during a data scan and recorded.

The watt-hour submeters, pyranometer, and the two heat flow measurements needed to be presented as integrated totals over a period of time. For this reason, the data from these associated sensors were digitized and summed using counters. In the case of watt-hour meters, a thin sector of each eddy disk was painted black to alter its reflectivity. The revolutions of the disk were counted by nearby optical sensors. This technique was entirely non-magnetic and caused no mechanical friction to the standard meter. The output of these sensors was digitized and sent to counters in the data acquisition system. In this way, the number of revolutions made by an eddy current disk in a watt-hour meter for any period of time could be revealed by reading the contents of the associated counter, and, knowing the K_h of the watt-hour meter, the number of Kilowatt-hours of energy for the period could be found.

Millivolt (D.C.) signals from the pyranometer were converted into digital signals through an analog-to-digital integrated circuit and sent to a counter in the data acquisition system. A data scan revealed the contents of

this counter indicating the integrated insolation for a period from when the counter was last zeroed.

Heat flow measurements consisting of the product of a calibration constant, a temperature difference ΔT, and a flowmeter output (see Equation 3-4) presented a special challenge. Not only must the signal appearing as heat flow data contain information from sensors T13, T14 and F2 (or T11, T12 and F1) but must also be directed to the proper counter in the data acquisition system to distinquish , for instance, between heat flow to space from the heat pump and heat flow to space from storage. Resolution of both of these problems is presented in Figure 16, showing the logic used for the heat flow station.

Two constant current supplies (CCS) provide 1 milliamp to each of the RTD's T13 and T14. The potential difference between points X and Y are proportional to the difference in temperature ΔT between these RTD's. This potential difference is fed to an analog-to-digital converter such that the frequency output of the A-D converter is proportional to ΔT. The flowmeter interface also produces a digital output of pulse width, W, proportional to the flowmeter output, FO. These two digital signals form the input to the gate AND1. AND gate logic is such that a +5 volt output is present only if all inputs are +5 volts, otherwise the output is 0 volts. Consequently AND1 produces an output frequency proportional to the product of the input frequencies, or more to the point, the output of

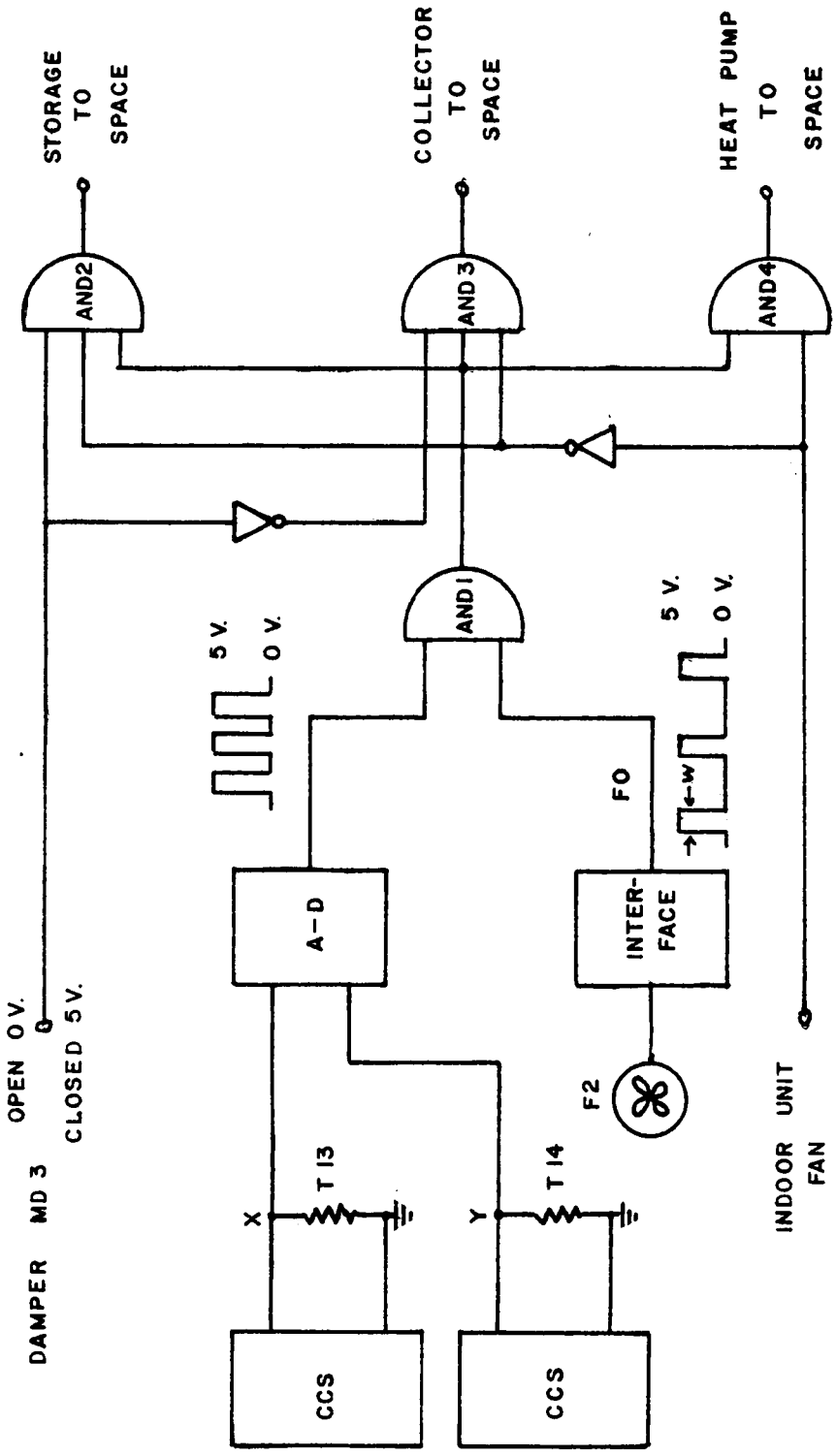


Figure 16. Heat Flow Measurement Logic.

AND1 is proportional to the product of FO and ΔT as desired. This output frequency indicates a heat flow to space that could occur when the system is in either of the modes (a) storage-to-space, (b) collector-to-space or (c) heat pump-to-space. Each of these modes is defined by a unique combination of the position of damper MD3 and the on-off state of the heat pump indoor unit. For example, an indicated space heat flow measurement while MD3 is closed and the indoor heat pump unit off could only mean that the system was in the storage-to-space mode rather than collector-to-space or heat pump-to-space modes. The uniqueness of the combined position of MD3 and the on-off state of the heat pump fan is exploited by the logic of the gates AND2, AND3, and AND4, as shown in Figure 16. In this way, space heat flow data from the heat pump can be distinquished between that from storage or that from the collectors, and can be routed to the proper counter in the acquisition system.

Collector heat flows measured by T11, T12 and F1 can be directed to storage or to space. AND gate logic based on that flow measurement and the position of damper MD4 provide the data acquisition a means of recognizing the mode of system operation at a particular time. There is so little difference between this logic circuit and the one in Figure 16, that it is not included here.

A summary of the data signals from the facility, and which arrive at the data acquisition system are listed with abbreviations as follows:

(1) Collector heat flow to space (COLSP)

(2) Collector heat flow to storage (COLST)

(3) Storage heat flow to space (STSP)

(4) Heat pump heat flow to space (HPSP)

(5) Electrical consumption of the solar air mover (SAMP)

(6) Electrical consumption of the heat pump indoor unit (HPIN)

(7) Electrical consumption of the heat pump outdoor unit (HPOD)

(8) Electrical consumption of the heat pump auxiliary heaters (HPAX)

(9) Electrical consumption of the offpeak heaters (OFFP)

(10) Total electrical consumption of the experimental facility

(11) Insolation as measured by the pyranometer

(12) Storage temperatures (T1 through T7)

(13) Space wet and dry bulb temperatures (T15 and T16).

Data signals (1) through (11) above are digital signals and each one integrated for one hour periods. The data signals (12) through (13) are analog.

The mainstay of the data acquisition system is a calculator with a 3.8 K word storage, printer and cassette tape unit. All digital signals are fed into a multiprogrammer where the raw data are converted to scaled

engineering units. At the time of an hourly scan, (a) analog signals are sequentially read by a digital voltmeter and also converted into scaled engineering units, (b) the contents of all counters are read, (c) the counters are reset to zero (d) a real-time copy of the scan is produced and (e) the accumulated data each hour is placed on magnetic tape. During the experiment, the magnetic data tapes were massaged by computer to produce weekly data summaries.

CHAPTER IV

SYSTEM PERFORMANCE

The very nature of this experiment required using those components which could be expected to perform reliably throughout the 1979-80 heating season. Missed data either due to component failure or instrumentation failure could not be recovered, so every effort was made to closely monitor the system and swiftly resolve problems as they arose. These efforts were rewarded when by the end of the data collection period on April 13, valid data had been collected continuously for 95% of the time since the experiment began. Contributing to the loss of data were problems associated with the system components as well as those associated with data acquisition.

Component Performance

While many of the operating system components functioned as expected, some did not. The collectors which were used had been tested by the manufacturer and shown to have a static pressure drop of 0.25 inches w.g. with a flow rate of 3.5 cubic feet per minute per square foot of collector area. Indications were that flow rates of 900 CFM could be expected with the collector array and air handler used. Upon installation and subsequent flow testing it was found that the 1/2 hp blower in the air mover could supply a flow rate of only 300 CFM through the

system in the COLSP mode. In this mode the static pressure drop in the collector array was measured to be .50 inches w.g. A 3/4 hp blower motor was then installed. The collector pressure drop rose to .60 inches w.g. and the flow rate to 400 CFM.

Ensuing discussions with the manufacturer revealed that their testing procedure had mistakenly placed the collector absorber under a positive static pressure, causing the absorber to "inflate" slightly, which reduced the pressure drop through the collector to the advertised value. The system was designed to have the collectors operate under a negative static pressure which caused the absorber plates to be drawn closer together thereby increasing the pressure drop. Increasing the fan size and power resulted in only modest gains in the flow rate. Small spacers were then installed in the collector absorber plenum to prevent its tendency to collapse. This modification reduced the pressure drop through the collector array and resulted in a flow rate of 700 CFM using the original 1/2 hp blower in the air mover. Aside from mechanical problems, the collectors were noticed to deteriorate slightly over this heating season. The inner cover of each collector is quite thin and serves to suppress convection losses. Due to thermal stresses, this cover ruptured in five of the twelve collectors used in the array. The resulting loss in thermal performance could only have been accurately determined by testing each

damaged collector, and this was not done. To do so would have meant interrupting the ongoing experiment.

The damper MD3 in the solar air mover often failed to fully open or fully close. This damper was operated by a small servo motor which rotated a pinion. The pinion meshed with a gear upon which the damper door was fastened. The damper was returned to the open position by a spring. At times, the damper would not close completely allowing air to simply recirculate within the air mover itself. Measurements revealed that 150 CFM of air were being recirculated whenever MD3 failed to close properly. It was felt that a more powerful motor would have consistently been able to close the damper against the return spring. However, a more powerful motor whose size did not exceed the space requirements was unavailable. The recirculation problem, though aggravating, did not prevent the remaining airflow from moving where intended, whether to space or storage.

During the night of November 30 when the outside temperature was 17°F, it was found that the heat pump was operating during the peak period even though there was sufficient thermal energy in storage to heat the facility directly. This observation pointed out a flaw in the offpeak control logic. During this cold period when the offpeak heater was on, the space temperature fell until the second stage of the thermostat engaged, turning on the heat pump. At the end of the offpeak period, the space heating

demand was such that the heat pump continued to operate, thereby preventing first stage of the thermostat from controlling the system, and directing stored heat to space. To correct this problem, a shunt on a 30 minute timer was placed across the outdoor anticipator of the heat pump, as shown in Figure 17. In the figure R10 is a small resistor in the indoor thermostat and R11 is a thermistor (outdoor anticipator), whose resistance rises with decreasing temperature. These two items are usually present to prevent thermostat droop. The timer provides a 30 minute "short" across R11 which causes more heat to be dissipated in R10. This heat causes enough of a rise in temperature within the thermostat to disengage the second stage bulb, turning off the heat pump and allowing the system to operate in the storage to space mode. This addition to the control strategy proved effective.

Data System Performance

All sensors used in the facility performed reliably for the duration of the experiment. Although the electronic data interfaces in the facility were protected from periods of reduced line voltage or surges by a power line conditioner and liberal shielding, electrical storms occasionally changed the contents of watt-hour and heat flow counters in the data acquisition system. In these cases, manual readings of the watt-hour meters were used to correct the recorded data, and excessive measured heat flows were discarded.

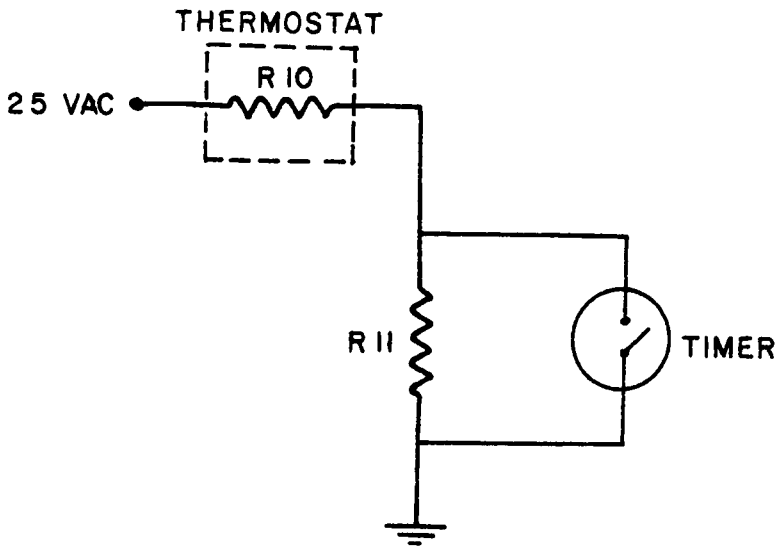


Figure 17. Offpeak Control Modification.

CHAPTER V

EXPERIMENTAL RESULTS

Data Analysis

It should be pointed out that the directly measured heat flows throughout the duration of the experiment in no way constitute all of the thermal paths that were possible. Losses of thermal energy can have a detrimental effect on the performance of a solar system especially if those losses are to the environment (17). Although in this experiment, all ducting and air moving devices were located in the conditioned space, calculations which would quantify all of the heat flows within the facility would prove helpful should one be faced with an installation which necessitated placing one or more components outside of the heated space. Such calculations were made for each hour of system operation and represent a major fraction of the data analysis.

All duct loss calculations were made by considering the air in the duct to be an ideal gas and using the expressions as follows:

$$\dot{Q} = UA\left[\frac{t_e + t_i}{2} - t_a\right] \qquad (5\text{-}1)$$

where

$$t_e = \frac{t_i(\gamma+1) - 2t_a}{\gamma - 1} \qquad (5\text{-}2)$$

and $$Y = \frac{28.8\, A^* \bar{V} \rho}{UA} \qquad (5\text{-}3)$$

In these expressions,

te = air temperature at duct entrance (^{o}F)

ta = ambient (room temperature,^{o}F)

A^* = cross-sectional area of duct (ft^2)

$\bar{V}$ = mean air velocity (ft./min.)

t_i = air temperature at duct exit (^{o}F)

U = overall coefficient of heat transfer (BTU/hr. ft.^{2} ^{o}F)

A = surface area of duct (ft.^{2})

$\dot{Q}$ = heat gain or loss through duct walls (BTU/hr.)

ρ = density of air (lbm./ft.^{3})

Quantities that were needed in the above list to calculate duct losses were either measured or calculated from available information. Although typical duct losses $\dot{Q}$, were noted to be very weak functions of air density ρ, the air densities in all ducting where a flow measurement was made were temperature corrected from the value of 0.075 lbm/ft.^{3}. Figure 11, page 28, shows a section of ducting between the calibration heater and sensor T11 which lost heat during the calibration procedure. The UA for this section of ducting was 4.25 BTU/hr.^{o}F giving a duct loss heat rate of 87 watts (0.78% of the energy supplied by the calibration heater). The uncorrected heat flows measured by the collector station were then multiplied by 1.0078

to give added accuracy. A similar correction was made for the space heat flow calibration. This heat flow calibration uses T13, T14, F2, and the heat supplied by the heat pump auxiliary and the indoor unit fan. Duct losses during this calibration amounted to 1.02% so that any heat flow measured into space was increased by the factor 1.0102. Appendix E lists the program which corrected the data and calculated all heat flows in the facility.

A block diagram of facility heat flows is shown in Figure 18. Since the 1/2 hp blower in the solar air mover (SAM) was located in the moving air stream, the energy dissipated by the blower contributed to the heat flow in four modes of system operation. The heat sources indicated in Figure 18 are as follows:

1. COLSP is the collected solar energy delivered directly to space when the system is operating as shown in Figure 8, page 21. This heat flow, measured by the collector heat flow station, was corrected to include duct losses which occur upstream from the station. The corrected heat flow includes the heat actually delivered to space through the supply duct as well as duct losses to space while the heated air is in transit to the supply duct.

2. COLST is the collected solar energy which is delivered to storage. COLST is the energy flow measured at the collector diminished by duct losses to space. This mode of operation is also shown in Figure 8, page 21.

3. SAM(COLSP) is the thermal energy from the solar

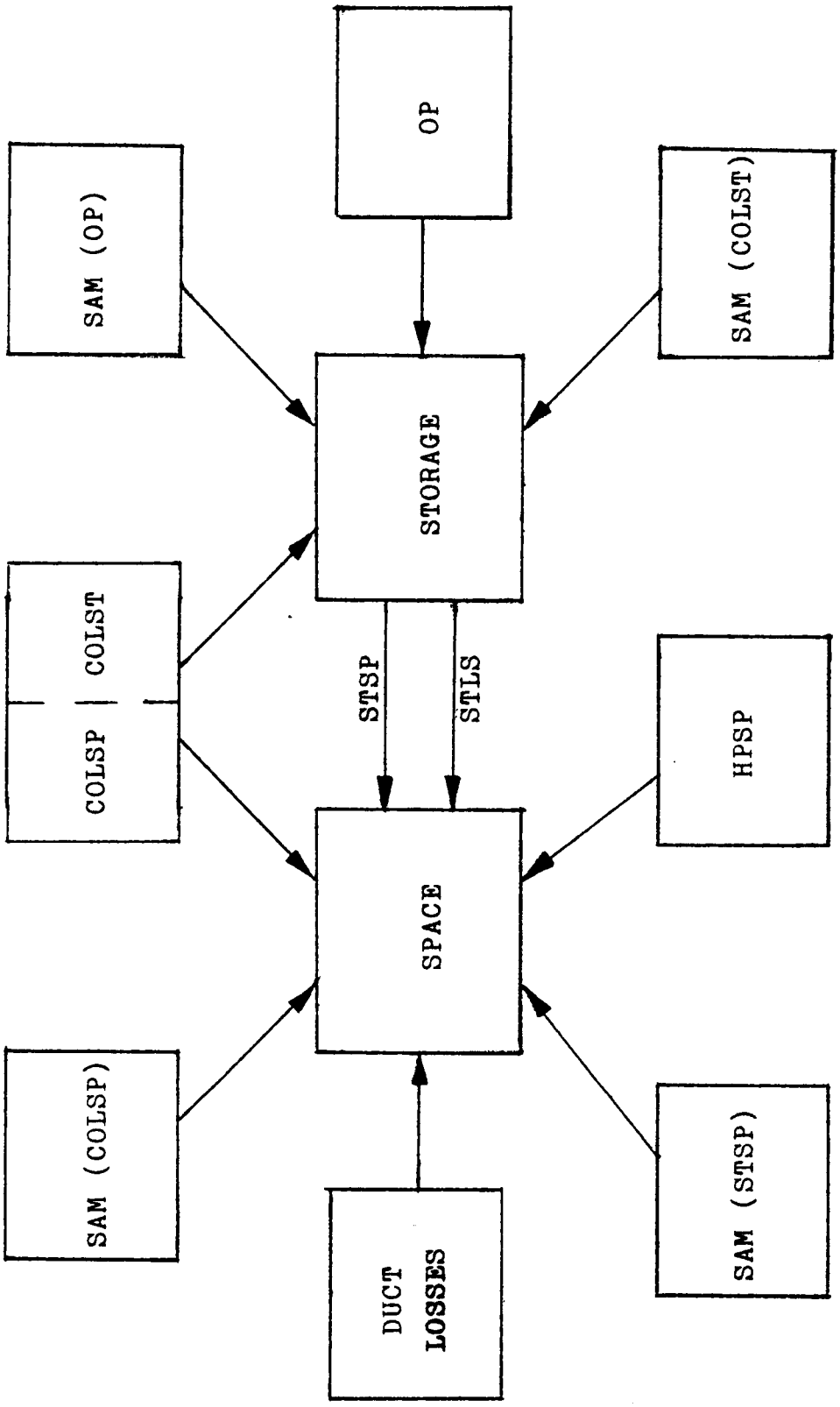


Figure 18. System Heat Flows.

air handler which arrives in space while the system is in the solar-to-space mode.

4. SAM(COLST) is the thermal energy from the SAM which winds up in storage when the system is in collector-to-storage mode.

5. STSP is the thermal energy that is removed from storage and sent to space, and is determined by data from the space heat flow measurement.

6. SAM(STSP) is the additional energy arriving in space due to the SAM when the system is in the storage-to-space mode shown in Figure 9, page 23. In this case, the space heat flow station senses both the heat flow from storage as well as the additional SAM energy.

7. OP is the electrical energy input to the offpeak heater minus the duct losses to space while the system is in the offpeak heating mode. In this way, OP is the heat energy from the offpeak heater that actually arrives in storage.

8. SAM(OP) is the thermal energy that the solar air mover blower contributes to storage during the offpeak period as shown in Figure 10, page 24.

9. STLS represents conduction losses through the walls of the storage box to space. These losses are determined by considering the storage walls to be a series of seven horizontal sections stacked together, with each section centered about one storage temperature measurement. For each section, a UA ΔT calculation determined the

continuous uncontrollable thermal losses from storage to space.

10. HPSP is the heat flow to space from the heat pump and the heat pump auxiliary, and is measured by the sensors at the supply and return ducts. HPSP includes both the measured heat flow to space and the unmeasured duct losses to space when the system is operating as shown in Figure 10.

11. DUCT LOSSES include those losses to space which have not been considered heretofore. There are 232 square feet of ducting between the collector outlet and sensor T12 and in the collector-to-storage mode this area magnifies conduction heat losses to space at the expense of collected energy to storage. DUCT LOSSES also include losses when the system is in the offpeak heating mode. In this case, not all of the electrical energy dissipated in the offpeak heaters arrives in storage. Some is lost to space.

Calculation of the above quantities each hour required knowing the length of time that the system was in any one mode. This determination was most accurately done by noting the electrical consumption each hour by the offpeak heater. A ratio between the offpeak electrical energy actually consumed in one hour to the maximum possible yielded the fraction of that hour in which the system was operating in the offpeak mode. The remaining portion of that hour could find the SAM either (a) off, (b) operating in solar-to-space mode, (c) operating in solar-to-storage

Table 1. System Energy Flows (KBTU).

	Nov05 to Dec02	Dec03 to Dec30	Dec31 to Jan27	Jan28 to Feb24	Feb25 to Mar23	Mar24 to Apr13	Total
COLSP	322.6	476.4	184.7	441.3	239.1	14.51	1678
COLST	3595	3381	1227	2261	2993	2194	15652
SAM(COLSP)	42.0	32.4	14.9	34.3	17.1	1.06	141.7
SAM(COLST)	325.4	222.3	101.6	183.1	265.5	220.5	1318
SAM(OP)	116.1	195.6	269.6	305.5	218.6	38.7	1144
SAM(STSP)	349.3	388.8	386.3	414.1	304.1	119.3	1962
DUCT LOSSES	493.6	682.3	569.1	988.6	707.2	397.9	3654
HPSP	891.2	1626	1761	3704	1878	19.9	9851
STLS	475.0	446.9	361.2	530.0	536.6	517.9	2848
OP	1604	3829	5431	5858	3696	653.3	21071
STSP	4750	7164	6953	8044	5975	2900	35134
Total heat to space	7291	10785	10230	13972	9658	3297	55234

comparative purposes. The period March 24 through April 13 however consists of only 21 days due to the termination of the experiment. These data indicate the expected results that as the middle of the heating season was approached, total heat sent to space increased, and the cycling of thermal energy to and from storage became more frequent. The total amount of heat sent to space for the period was 55234 KBTU. Of this amount, 3% was sent directly to space from the collectors, and 28% arrived in space only after being cycled through storage. Approximately 8% of the heat passing into space came from the blower in the SAM, indicating the advantage of having the SAM motor in the air stream rather than external to the housing, and located outside the conditioned space. The fact that all thermal flows terminate in the conditioned space is beneficial to the heating system performance in the experimental facility. Conduction losses from storage combined with the duct losses in the collector-to-storage and offpeak to storage modes comprise 12% of the heat delivered to space. If both storage and the offpeak heater loop had been located in an unheated basement, even more heat would be lost due to a lower ambient temperature surrounding the storage and offpeak ducting. If these components were in a 50°F basement, rather than a 68°F room, typical losses would be approximately 20%.

The building heat load characteristics were studied by calculating for each week of the experiment, the building

heat load coefficient. This coefficient is defined as the rate at which heat is delivered to space divided by the average temperature difference between the ambient and the building dry bulb temperatures. Figure 19 shows the results of this calculation plotted against outdoor dry bulb temperature. The building heat load coefficient was defined for this plot to indicate the heat needed by a building exclusive of internal energy gains generated within to maintain the space temperature at 68°F. Particularly at higher outside temperatures, the heat load coefficient is substantially reduced as the interior loads were able to supply an increasingly larger fraction of the space heat. If the internal energy gains due to the load simulator are included in the total heat delivered to space, the building heat load coefficient was significantly higher. At an ambient temperature of 24°F, the heat load coefficient was measured to be 790 BTU/hr.°F. If the ambient temperature was 48°F, the heat load coefficient was reduced to 628 BTU/hr.°F. This variation in heat load coefficient was not unexpected. During colder weather, larger pressure differences existed between the ceiling and outside the roof resulting in a "chimney effect" which increased the infiltration rate. A detailed building heat load calculation shown in Appendix B indicates a constant heat load coefficient of 1040 BTU/hr.°F. The discrepancy between the load calculated in Appendix B and the measured value are in part due to the large roof area covered by the

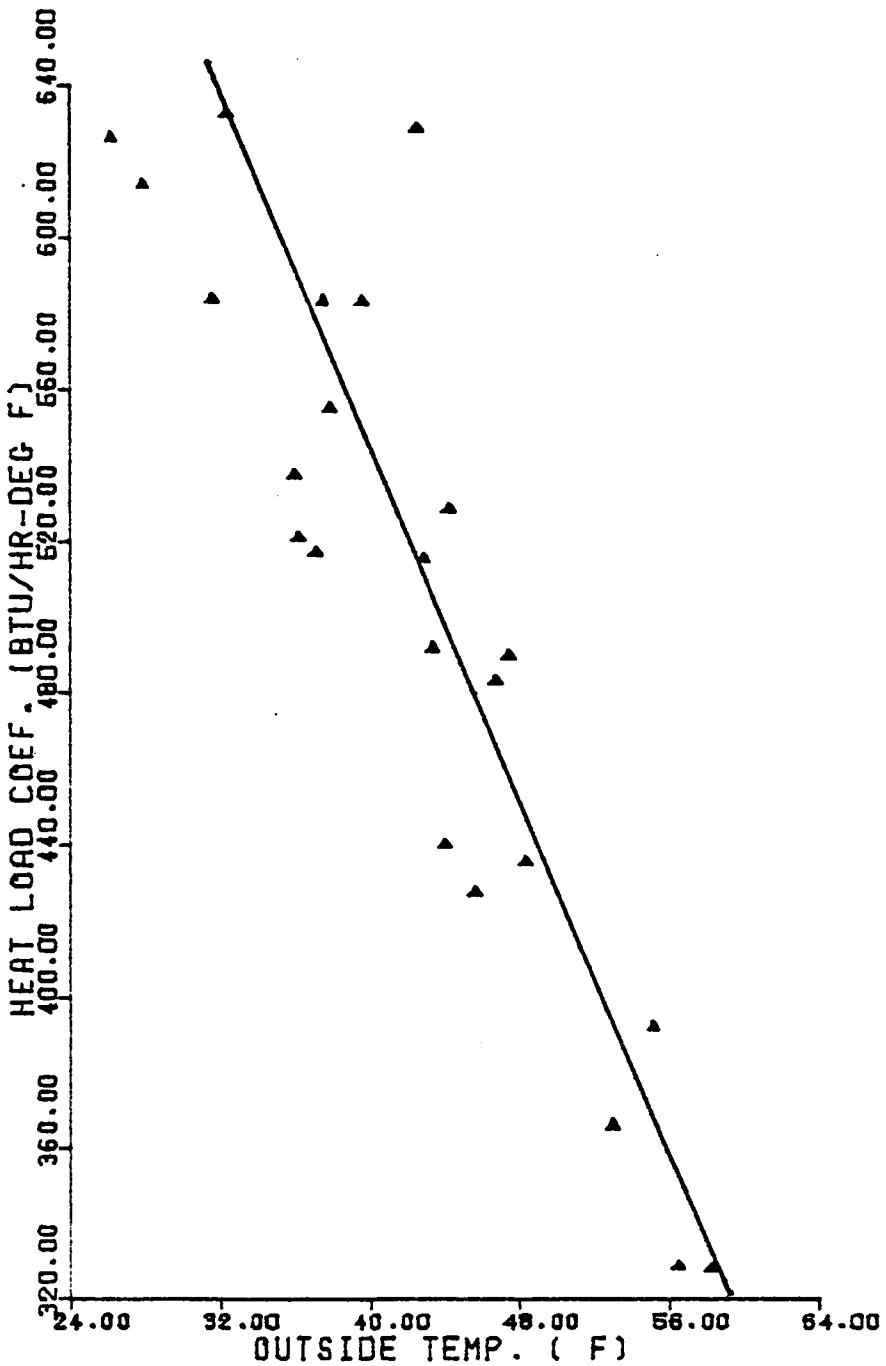


Figure 19. The Building Heat Load.

collector array. Apparently the presence of this collector array serves to suppress conduction losses below those which would be present if the roof surface had been conventional and exposed to still air, as assumed in Appendix B.

To quantify the collector array performance, a determination was made of the hourly efficiency for a 12-hour period. The ambient temperature during the day of February 4 averaged 24 °F, and the insolation was high. This meant that the heating demand of the building was large and that this demand was at least partially met by solar. During this day, the SAM ran continuously in the solar-to-space and solar-to-storage modes. This was a necessary requirement in the determination of array efficiency due to the hourly nature of data collection. Figure 20 indicates the collector performance. The efficiencies were simply the ratio of solar energy delivered to space and storage to the accumulated hourly insolation. The maximum hourly efficiency on this day was 46% which was maintained for two hours. Insolation values were approximately the same from 9 to 10 A.M. and 4 to 5 P.M. (EST), yet the amount of solar energy collected in the afternoon was four times that collected in the morning. Although thermal lag accounts for some of this difference, partial shading of the collector array in the morning due to an adjacent building constitutes the remainder.

The purchased electrical energy requirements during

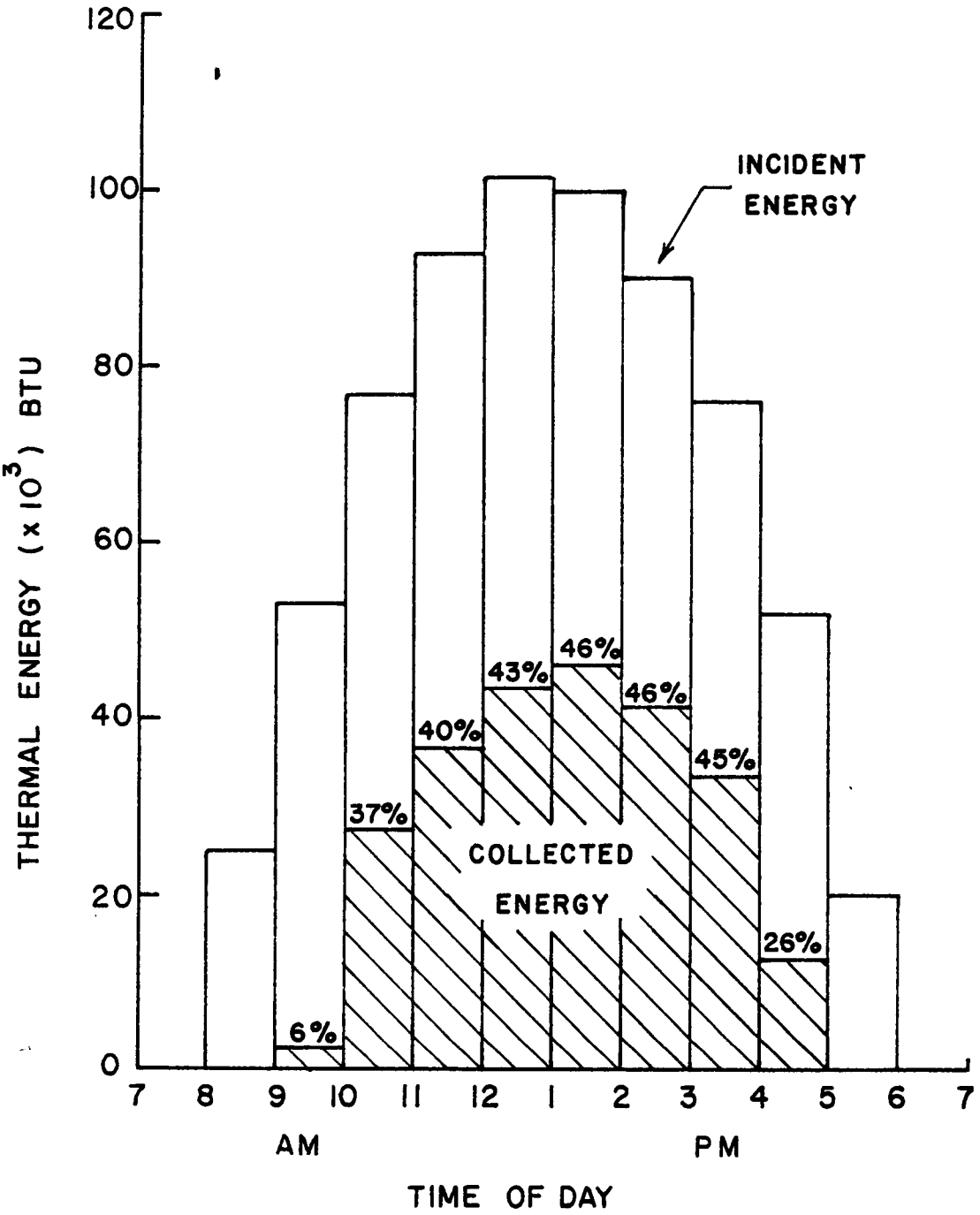


Figure 20. Collector Performance on February 4.

the experiment are listed in Table 2, where (a) HPIN represents the indoor heat pump unit fan, (b) HPOD represents the outdoor heat pump unit, (c) HPAUX represents the auxiliary heat, (d) SAM, the solar air mover, (e) INT, the interior load simulator, (f) OFFPK, the total energy consumed by the offpeak heater, (g) TONPK, the total electrical energy delivered to the facility during the onpeak periods, and (h) TOFFPK is the total electrical energy delivered during the offpeak period.

Table 2. Facility Electrical Energy (KBTU).

	Nov05 to Dec02	Dec03 to Dec30	Dec31 to Jan27	Jan28 to Feb24	Feb25 to Mar23	Mar24 to Apr13	Total
HPIN	49.76	87.38	94.02	202.4	87.03	1.08	521.7
HPOD	445.0	680.2	739.5	1321	605.6	105.3	3897
HPAUX	95.39	150.9	82.10	648.8	661.7	.02	1638
SAM	826.1	839.2	772.2	937.0	805.4	379.2	4559
INT	2661	2646	2252	2084	1375	1562	12580
OFFPK	1724	4123	5846	6316	3983	703.2	22695
TONPK	1583	1546	1156	1434	1221	781.8	7722
TOFFPK	4218	6981	8630	10076	6297	1969	38171

The drop in the internal loads beginning February 25 was due to a decrease in the lighting load inside the building. Other variations were caused periodically by occupants and associated testing.

For this experiment, the winter peak periods were taken to be 7 A.M. to 1 P.M. and 6 P.M. to 10 P.M. (EDT) weekdays. Although the offpeak controls were set to allow the offpeak heaters to operate each day of the week, all weekend usage was designated offpeak.

Using these offpeak and onpeak periods, of the 45,893 KBTU (or 13446 Kw-hr) of electricity used during the experiment, 38171 KBTU (or 11184 Kw-hr) were used during offpeak times, thus yielding an offpeak fraction of 83%.

Performance coefficients for the system and components were also determined both weekly and for the season. Using the data collected and associated symbols, the heat pump coefficient of performance is taken as the ratio,

HPSP/(HPIN + HPOD + HPAUX).

The performance of the solar system was assessed by taking the ratio of (a) the energy delivered to space by the solar system to (b) the parasitic energy required, or the solar performance factor was calculated by dividing

SOLST + SOLSP + SAM(COLSP) + SAM(COLST) + SAM(STSP)

by the quantity

SAM(COLSP) + SAM(COLST) + SAM(STSP).

In this case, the solar air mover not only provided the work needed to move solar energy ultimately into space, but also contributed heat to the space itself. Finally the overall system performance was determined. This ratio simply compares the total heat energy actually sent to space, to the energy which was purchased. Obviously, pure

resistance heating would have a system performance factor of one. Table 3 shows these performance factors in a weekly format. The heat pump seasonal COP was demonstrated to be 1.62. The seasonal solar COP was 9.43 and the seasonal system performance, 1.66. Although the seasonal system performance is only 66% greater than that for pure resistance heating, offpeak rates could make the system economical.

The seasonal operational costs of a space heating system depend both on the purchased energy costs and the amount of purchased energy used. A comparison of these operating costs requires the following definitions:

ON = cost / energy unit purchased onpeak

OFF = cost / energy unit purchased offpeak

F = fraction of energy purchased offpeak

TH = total heat delivered to space for the season

SPF = total heat delivered / total purchased energy.

Using these definitions, it is apparent that,

total energy purchased = TH/SPF

total energy purchased offpeak = (F)(TH/SPF)

total energy purchased onpeak = (1 - F)(TH/SPF).

The seasonal costs, $, would then be

$$\$ = (ON)(1 - F)(TH/SPF) + (OFF)(F)(TH/SPF)$$

or,

$$(SPF)(\$/TH) = ON - (F)(ON - OFF). \qquad (5\text{-}4)$$

Equation 5-4 indicates that a reduction in $/TH is always a result of an increase in SPF. In addition, if time-of-day

Table 3. Weekly Performance Factors.

DATE (WEEK BEGINNING)	AVERAGE OUTDOOR DRY BULB TEMPERATURE(°F)	HEAT PUMP COP	SOLAR COP	SYSTEM COP
Nov. 5	48.3	0.31	6.46	1.59
Nov.12	44.0	1.37	8.49	1.84
Nov.19	56.4	.00	8.04	2.06
Nov.26	37.9	1.75	9.29	1.77
Dec. 3	36.0	1.66	12.55	1.84
Dec.10	42.9	1.78	9.13	1.60
Dec.17	37.1	1.73	10.77	1.60
Dec.24	39.6	1.83	9.75	1.31
Dec.31	36.2	1.95	9.21	1.33
Jan. 7	37.5	2.00	8.13	1.13
Jan.14	45.6	1.46	9.60	1.28
Jan.21	42.5	1.94	9.97	1.26
Jan.28	26.2	1.68	10.00	1.30
Feb. 4	27.9	1.84	10.35	1.26
Feb.11	31.6	1.72	10.42	1.58
Feb.18	46.7	1.43	10.84	1.58
Feb.25	32.4	1.39	9.86	1.47
Mar. 3	43.3	1.41	10.58	1.70
Mar.10	44.2	1.40	9.15	1.58
Mar.17	47.4	1.26	9.46	1.49
Mar.24	52.9	0.45	8.22	1.42
Mar.31	55.1	0.05	9.84	2.28
Apr. 7	58.2	.00	9.24	2.21

rates are used, a reduction in $/TH would occur with an increase in the offpeak fraction, F. Equation 5-4 is plotted in Figure 21 and compares the seasonal costs for three systems using time-of-day pricing. System (A) is the experimental offpeak heating facility with an offpeak fraction of 0.83 and system performance factor of 1.66 as determined from the experimental data. System (B) is a house with resistance heating only and no storage capability. The offpeak fraction for this house was assumed to be 0.66, a typical value for a residence in the TVA valley (4). System (C) is a house with a heat pump and no storage. The seasonal heat pump COP for system (C) was assumed to be 1.62 which was the demonstrated COP during the experiment. The offpeak fraction was again assumed to be 0.66. Figure 21 indicates, for example, that if onpeak rates were $.07 per Kw-hr and offpeak $.03 per Kw-hr, the seasonal cost per heat unit delivered to space by the experimental offpeak system would be $.022 per Kw-hr. With the same rate structure, the cost for system (B), the resistively heated house, would be $.045 per Kw-hr, while the cost for system (C) would be $.027 per Kw-hr. An electrical utility which experiences a severe winter peaking problem would probably incorporate into its rate structure significant differences in on and offpeak prices. If onpeak rates were $.09 per Kw-hr and offpeak $.01 per Kw-hr, seasonal costs per heat unit for system (A) would be $.0142, for system (B), $.0372 and for system (C), $.023.

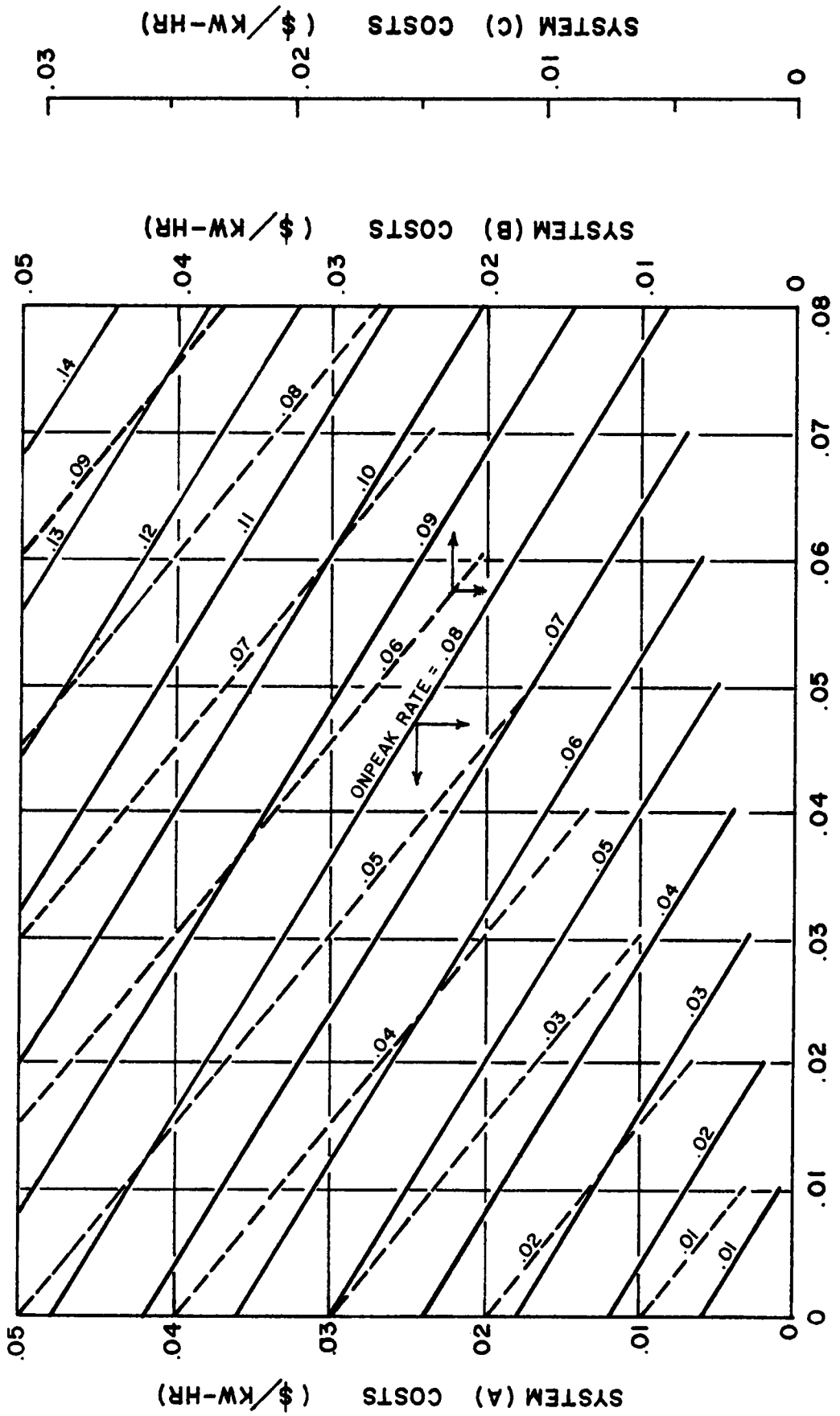


Figure 21. Time-of-Day Rate Comparisons.

This indicates that system (A) requires only 38% of the purchased energy needed by system (B) and 62% of that needed by system (C). Although operating costs of the experimental heating system are clearly the least expensive of the three systems compared, the additional capital costs of system (A) might not make that system the most economical choice. Offpeak rates currently being considered in the TVA region are $.0382 onpeak and $.0142 offpeak (4). If electricity were sold at this rate, Figure 21 indicates that system (A) would cost $.011 and system (C) would cost $.013 per Kw-hr of heat delivered to space. Since the heating system delivered 55234 KBTU (16183 Kw-hr) to space, the seasonal costs for system (A) would be $178 and for system (C), $210. Systems (A) and (C) would have the same seasonal operating costs with this rate structure if the average COP of the heat pump were 2.03, and system (C) would operate more economically than (A) if the COP were greater then 2.03.

Conclusions

This experiment has demonstrated the reductions in peak electrical demand which are possible using offpeak heating. An offpeak fraction of 0.83 and seasonal performance coefficient of 1.66 were obtained during the 1979-80 heating season. Due to the stipulated requirement of minimal onpeak electrical usage and resulting system design, it is felt that the offpeak fraction obtained

represents a maximum for the facility. The large offpeak fraction coupled with the measured seasonal performance coefficient can give the system a distinct advantage with time-of-day pricing of electricity.

Recommendations

Although the data system operated for the most part as designed, measurement techniques for sensing air-side heat flows could be improved. This would necessitate direct determination of heat flows using flow rate, air properties in the duct and temperatures. By using sensors to obtain a heat flow constant as was done, measuring heat flows relying on that constant compounds errors in the final result.

A more accurate determination of collector performance would dictate locating the pyranometer as near the collector as possible, so that differences in what the pyranometer and collector array "sees" are minimized.

If a monitored temperature measurement had been made at the outlet from the collector, more accurate calculations for duct losses could have been made, and instantaneous collector efficiencies could have been determined.

It was essential in the experiment to optimize the system so that even with offpeak rates, no more electricity than necessary would be used by the offpeak heater. It would be desirable to couple the storage of offpeak energy

to future insolation conditions. In the present system, the amount of electricity used to charge the depleted pebble bed was determined by using thermostatic controls which sensed outdoor temperature and pebble bed temperatures at two locations. This type of storage pre-charging control system does not always charge storage to an "optimal" amount (defined here as the minimum offpeak electrical energy required to ensure that no additional electricity would be required during the peak periods of the next day). Dynamic controls would integrate weather and load forecasts with existing information on thermal storage "charge levels" to determine optimal back up pre-charge. When insolation and low thermal loads are anticipated, pre-charge would be decreased and vice-versa. It is recommended that control systems be investigated which not only sense outdoor temperature, but levels and changes in barometric pressure which quite often indicate increasing insolation levels.

It is obvious in the experiment, that the heat pump provided back up heat only when storage was depleted or being charged by the offpeak heater. Design specifications prevented the heat pump from operating during onpeak times. While this requirement served to increase the offpeak fraction, it also reduced the system performance. Allowing the heat pump to be used in a less restrictive way through a redesign of the controls would reduce the offpeak fraction, but also raise the system performance

coefficient. This mode of operation could reduce seasonal heating costs even more particularily under a rate structure with a moderate difference in off and onpeak rates.

LIST OF REFERENCES

LIST OF REFERENCES

1. TVA Report on Ratemaking Standards. Tennessee Valley Authority, Office of Power (December 1979).

2. Asbury, J.; Giese, R.; Nelson, S.; Akridge, L.; Graf, P.; and Heitner, K.; "Assessment of Energy Storage Technologies and Systems (Phase I): Electric Storage Heating, Storage Air Conditioning, and Storage Hot Water Heaters." Argonne National Laboratory Publication No. ANL/ES-54, (October 1976).

3. "Survey of Utility Load Management and Energy Conservation Projects Part I, Final Report." Energy Utilization Systems, Incorporated, prepared for Oak Ridge National Lab, publication No. ORNL/Sub-77/13509/2, (December 1977).

4. Knoxville Residential Time-of-Day Rate Test. Tennessee Valley Authority, Office of Power, (December 1979).

5. Hughes, P.; Duffie, J.; and Beckman, W.; "Simulation Study of Several Heating Systems with Off-Peak Auxiliary." Solar Energy 19 (1977):317-319.

6. Karman, V.; Freeman, T.; and Mitchell, J.; "Simulation Study of Solar Heat Pump Systems." a paper presented at the Sharing the Sun Conference, Winnipeg, Canada, (August 1976).

7. Converse, A., "Solar Heating in Northen New England." a paper presented at the Sharing the Sun Conference, Winnipeg, Canada, (August 1976).

8. Freeman, T.L.; Mitchell, J.W.; and Audit, T.E.; "Performance of Combined Solar-Heat Pump Systems." Solar Energy 22 (1979): 125-134.

9. Morehouse, J.H.; and Hughes, P.J.; "Residential Solar Heat Pump Systems: Thermal and Economic Performance." ASME Paper Number 79-WA/SOL-25, 5-6, (August 1979).

10. Solar Heating and Cooling of Residential Buildings - Sizing, Installation and Operation of Systems, prepared by the Solar Applications Laboratory, Colorado State University, Department of Commerce publication number 003-011-00085-2, (January 1977): 6-5.

11. Latimer, J.R.; "Radiation Measurement." Technical Manual Series Number 2, Canadian National Committee for the International Hydrological Decade, Ottawa, Canada, (1971).

12. Test No. S100-4, Test Report, Metrology Research and Development Laboratory, ORNL, (July 1979).

13. Test No. S100-3, Test Report, Metrology Research and Development Laboratory, ORNL, (July 1979).

14. Cornwall, Brian. Airflow Development Limited, Toronto, Canada. Interview, 21 May 1980.

15. Blevins, Don P. Knoxville Utility Board, Knoxville, Tennessee. Interview, 12 May 1980.

16. Strock, Clifford, and Koral, Richard, ed. Handbook of Air Conditioning and Ventilating. New York: Industrial press, Inc., second edition, (1975): 2-94.

17. Beckman, W.A.; "Duct and Pipe Losses in Solar Energy Systems." Solar Energy 21 (1978): 531.

18. ASHRAE 1977 Fundamentals, published by the American Society of Heating, Refrigerating, and Air Conditioning Engineers, Incorporated, third printing, New York (1978): 31.10.

19. Kline, S.J.; and McClintock, F.A.; "Describing Uncertainties in Single-Sample Experiments," Mechanical Engineering 75, No. 1, (January 1953): 3-8.

APPENDICES

APPENDIX A

FACILITY COMPONENT DESCRIPTION

Collectors: Westinghouse model NSW-A-480

Solar air handler: Solar Control Corporation model SAM-10A

Heat pump: Westinghouse Hi/Re/Li System,
outdoor unit, model HP030D
indoor unit, model AH012H

Indoor thermostat: custom made by General Electric for Westinghouse, Westinghouse model 3AAT80

Offpeak heater: Electric Heaters Incorporated model IN1818-15-2NFTAL-230-24

Pyranometer: Eppley Black and White model 8-48

Storage RTD: Minco model S53P360Y6

Heat flow RTD: Minco model S1107-1

Turbine flowmeter: Davis model EDRA

Space temperature probe: Analog Devices model AC2626L4SS

Data acquisition system:
Hewlett-Packard calculator model 9825A
Hewlett-Packard multiprogrammer model 6940B
Hewlett-Packard digital voltmeter model 3455A

APPENDIX B

BUILDING HEAT LOAD CALCULATION
(ASHRAE, Reference 18, Section 22)

Roof - shingled plywood

	exposed portion:	covered portion:
area (sq. ft.)	561.00	400.00
inside surface resistance	0.62	0.62
5/8 inch plywood resistance	0.78	0.78
shingle resistance	0.44	0.44
outside surface resistance	0.17	0.62
Total resistance	2.01	2.46
Transmission coefficient	.498	.407

$Qr/(Ti-To) = (.498)(.561) + (.407)(400) = 442$ BTU/hr.°F.

Wall - sheathed stud wall, plywood exterior, sheet rock interior, area of 651 sq. ft.

	between framing:	at framing:
inside surface resistance	0.68	0.68
1/2 inch sheet rock	0.45	0.45
air space	1.01	--
2 X 4 inch stud	--	4.38
3/4 inch sheathing	2.20	2.20
5/8 inch plywood	0.78	0.78
outside surface resistance	0.17	0.17
Total resistance	5.29	8.66
Transmission coefficient	.189	.155

Using a 20% framing factor,
$Qw/(Ti-To) = (.2\ (.115) + .8\ (.189))\ (651) = 113$ BTU/hr.° F.

Gable - sheathed stud wall, plywood exterior, area of of 309 sq. ft.

	between framing:	at framing:
inside surface resistance	0.68	0.68
2 X 4 inch stud	--	2.19
3/4 inch sheathing	2.20	2.20
5/8 inch plywood	0.78	0.78
outside surface resistance	0.17	0.17
Total resistance	3.83	6.02
Transmission coefficient	.261	.166

Using a 40% framing factor,
$Qg/(Ti-To) = (.4\ (.166) + .6\ (.261))\ (309) = 69$ BTU/hr.°F.

Garage Door - folding, made of hardboard, area of 118 sq. ft.

inside surface resistance	0.68
1/4 inch hardboard	0.34
outside surface resistance	0.17
Total resistance	1.19
Transmission coefficient	.84

$Qgd/(Ti-To) = (.84)(.118) = 99$ BTU/hr.°F.

Entrance Door - solid core wood, area of 20 sq. ft.

inside surface resistance	0.68
1.5 inch solid core wood	1.80
outside resistance	0.17
Total resistance	2.65
Transmission coefficient	.377

$Qd/(Ti-To) = (.377)(20) = 7.5$ BTU/hr.°F.

Overhang - plywood, area of 135 sq. ft.

inside surface resistance	0.92
5/8 inch plywood	0.78
outside surface resistance	0.17
Total resistance	1.87
Transmission coefficient	.53

$Qo/(Ti-To) = (.53)(135) = 71.5$ BTU/hr.°F.

Floor - 4 inch concrete slab on grade, perimeter of 98 ft., edge factor of .81

$Qf/(Ti-To) = (.81)(98) = 79$ BTU/hr.°F.

Infiltration - assuming one air change each hour, building volume of 9000 cubic ft.

$Qi/(Ti-To) = (0.018)(1)(9000) = 162$ BTU/hr.°F.

Total Heat Load

$$Qt = Qr + Qw + Qg + Qgd + Qd + Qo + Qf + Qi$$

or

$Qt/(Ti-To) = 1043$ BTU/hr.°F.

APPENDIX C

OFFPEAK CONTROL THERMOSTAT SETTINGS

Given:

Conservative projection of offpeak heating load:
500 BTU/hr.°F
Design temperature: 17°F
Inside space temperature: 68°F
Thermostat T1 located in the middle of storage adjacent to T7
Thermostat T3 located adjacent to T8
Storage mass: 26000 lbm
Storage specific heat: 0.2 BTU/lbm°F

A.

In 6 hours, at design conditions the building will lose
(500 BTU/hr. °F)(6 hr.)(68°F-17°F) = 153,000 BTU.
The time needed to charge storage using the 15 KW offpeak heater is,
time = (153,000 BTU/15 KW)(1 KW-hr./3414 BTU)
= 3 hours.
Thus the offpeak timer was set for 3 hours.

B.

The 10 KW offpeak heater will supply 102,400 BTU to storage during this 3 hour period, changing the average storage temperature by 20°F. If this energy is to be lost by the building in 6 hours, then the minimun outside temperature, To, is found as follows:
(6 hr.)(500 BTU/hr.° F)(68°F-To) = 102,400 BTU
or To = 34°F. Thus the outdoor thermostat was set to 34°F.

C.

With the outdoor temperature 34°F, heat must be sent from storage to space at a minimun rate of 17000 BTU/hr. to maintain 68°F inside the building. This requires a minimum air delivery temperature from the top of storage found by,
Q = C (air flow rate) (ΔT)
where, Q = 17000 BTU/hr.
C for air = 1.08 BTU/(cfm hr.° F)
air flow rate = 700 cfm
T = Tmin - 68°F.
This gives a minimum top storage temperature of 90°F.

Since the storage bottom remains at 68°F, the following results can be seen:

	Charged storage	Depleted storage
Bottom storage temperature	68°F	68°F
Top storage temperature	--	90°F
Average storage temperature	99°F	79°F
Storage temperature at T1	99°F	79°F

Thus thermostat T1 in the middle of storage was set to 99°F.

D.

The 15 KW offpeak heater supplies 153,000 BTU to storage during the 3 hour charging period and raises the average storage temperature by 29°F. An analysis similar to part (C) indicates a minimum top storage temperature of 102°F is required. Noting that T3 is located one-third of the distance from the middle to the bottom of storage, the following results can be deduced:

	Charged storage	Depleted storage
Bottom storage temperature	68°F	68°F
Top storage temperature	--	102°F
Average storage temperature	114°F	85°F
Storage temperature at T3	98°F	79°F

Therefore thermostat T3 was set to 98°F.

APPENDIX D

EXPERIMENTAL ERROR ANALYSIS

A. Electrical Energy Consumption Uncertainty

Each sensor used in the experiment has an uncertanty and contributes to the overall experimental uncertainty of the results. The watt-hour submeters used had been recently calibrated to within 0.5%, and since the electrical usage is cumulative over each hour and the manner in which these meters were read by the data system used digital counting, the uncertainty in electrical energy consumption by any of the submetered components remains at 0.5%.

B. Heat-flow Uncertainty

The method used to measure heat flows in the system requires that an error analysis be carried out for the calibration process to obtain an uncertainty in the calculated calibration constant, the expression on the right hand side of Equation (3-5). The resulting uncertainty in the calibration constant then is propagated into any calculation using Equation (3-4) to determine heat flow. The generally accepted method (19) of error propagation is used to arrive at an overall heat flow uncertainty.

The calibration procedure required that the following data be taken while the calibration heater was on, and the system in COLST mode. The symbol, w, is the uncertainty.

Watt-hour meter

$K_h = 3.6$	$w_{K_h} = .018$	(0.5%)
Time, T = 120 sec.	$w_T = 1$ s	
Revolutions, R = 100	$w_R = 0$	

Temperatures

T11 = 70°F	$w_{T11} = 1.8$°F	(2.5%)
T12 = 155°F	$w_{T12} = 3.9$°F	(2.5%)

Flowmeter

FO = 560 counts	$w_{FO} = 17$ counts	(3.0%)

To find the power input to the heater,

$$Q = ((K_h)(R))/T = 10{,}800 \text{ watts}$$

The uncertainty in $\dot{Q}$ is found from:

$$w_{\dot{Q}} = \left[\left(\frac{\partial \dot{Q}}{\partial k_h} w_{k_h}\right)^2 + \left(\frac{\partial \dot{Q}}{\partial R} w_R\right)^2 + \left(\frac{\partial \dot{Q}}{\partial T} w_T\right)^2\right]^{1/2}$$

$$= 105 \text{ watts}$$

$$\therefore \quad \dot{Q} = 10{,}800 \pm 105 \text{ watts}$$

From Equation (3-5), $K' = \rho C_p KA = \dot{Q}/((FO)(T12-T11))_{CAL}$

$$= \dot{Q}/((FO)(\Delta T))_{CAL} = .22689$$

The uncertainty in K' is found using

$$w_{K'} = \left[\left(\frac{\partial K'}{\partial \dot{Q}} w_{\dot{Q}}\right)^2 + \left(\frac{\partial K'}{\partial FO} w_{FO}\right)^2\right]^{1/2},$$

so that $W_{K'} = .00723$

$$\therefore \quad K' = .22689 \pm .00723$$

To find the uncertainty in heat flow, then

$$\dot{Q} = (K')(FO)(\Delta T)(B)$$

where $B = \rho C_p / (\rho C_p)_{CAL}$

The factor B accounts for the possibility of differences in ρC_p between the calibration and data collection periods. Since this variation could be 3%, B = 1 and $W_B = .03$, and

$$w_{\dot{Q}} = \left[\left(\frac{\partial \dot{Q}}{\partial K'} w_{K'}\right)^2 + \left(\frac{\partial \dot{Q}}{\partial FO} w_{FO}\right)^2 + \left(\frac{\partial \dot{Q}}{\partial B} w_B\right)^2\right]^{1/2}$$

$$= 575.2$$

Therefore, a measured heat flow rate of 10,800 watts becomes

$$\dot{Q} = 10{,}800 \pm 575.2 \text{ watts}$$

This indicates that the measured heat flows have an approximate error of 5.3%.

APPENDIX E

DATA ANALYSIS COMPUTER PROGRAM

```
      DIMENSION T(32),F(32),Q(3),TA(3),TSP(3),WSP(3),
      1DELQ(3)
      DO 100 J=1,32
100   F(J)=1.0
C  DATA CORRECTION FACTORS MAY BE INPUT BELOW:
      F(3)=1.027
      F(26)=1.0105
      F(27)=1.0105
      F(28)=1.0078
      F(25)=1.0078
C*********************************
      L=3
      TCAP=0.0
      K=0
      DK=0.
      STOL=0.0
      EN=0.0
      TSUN=0.0
      TOTDL2=0.0
      TOTDL5=0.0
      SOLCOT=0.0
      HPSP=0.0
      ONPK=0.0
      OFFPK=0.0
      HPAX=0.0
      HPIN=0.0
      HPOD=0.0
      SAME=0.0
      OPT=0.0
      CEMAX=0.0
      SSTSP=0.0
      SSCSP=0.0
      SSCST=0.0
      TSOLST=0.0
      TSOLSP=0.0
      SOP=0.0
      OPST=0.0
200   FORMAT(I5/I5/I1/I2)
      READ(5,200) ISTART,ISTOP,IDAY,IHOUR
      INT=ISTOP-ISTART
      OPEN(UNIT=40,DIRECTORY='22665,212266')
250   READ(40,255) II,(T(I),I=2,8)
255   FORMAT(I10,7E10.4)
300   FORMAT(8E10.4)
```

```
      IF(II.GE.ISTART) GO TO 500
      READ(40,400) SKIP
400   FORMAT(E10.4//)
      IHOUR=IHOUR+1
      IF(IHOUR.LT.24) GO TO 450
      IHOUR=0
      IDAY=IDAY+1
      IF(IDAY.GT.7) IDAY=1
450   GO TO 250
500   DO 1000 M=1,INT
      READ(40,300) (T(I),I=9,16)
      READ(40,300) (T(I),I=17,24)
      READ(40,300) (T(I),I=25,32)
C  SUN=SOLAR ENERGY (BTU) FALLING ON COLLECTORS HOURLY.
      SUN=T(3)*F(3)*29.43*3.413
C  TSUN=TOTAL SOLAR ENERGY FALLING ON COLLECTORS (BTU) FOR PERIOD
      TSUN=TSUN+SUN
C  CORRECTIONS FOR DROPPED DATA (ANALOG)
      IF(T(17).LE.50.0) T(17)=100.0
      IF(T(18).LE.50.0) T(18)=95.0
      IF(T(19).LE.50.0) T(19)=91.0
      IF(T(20).LE.50.0) T(20)=87.0
      IF(T(21).LE.50.0) T(21)=83.0
      IF(T(22).LE.50.0) T(22)=78.0
      IF(T(23).LE.50.0) T(23)=72.0
      IF(T(7).LE.50.0) T(7)=68.0
      IF(T(8).LE.30.0) T(8)=50.0
C  DIGITAL DATA WARNINGS FOLLOW:
5000  IF(T(3).EQ.-.1000E-08) GO TO 5002
      GO TO 5006
5002  WRITE(L,5004) II, IHOUR, IDAY
5004  FORMAT('0',3X,'INSOLATION AT TIME=',I10,3X,
     1'HOUR= ',I2,3X,'DAY= ',I1)
5006  IF(T(11).EQ.-.1000E-08) GO TO 5012
      GO TO 5016
5012  WRITE(L,5014) II, IHOUR, IDAY
5014  FORMAT(' ',3X,'HP AUX AT TIME=',I10,3X,
     1'HOUR= ',I2,3X,'DAY= ',I1)
5016  IF(T(12).EQ.-.1000E-08) GO TO 5022
      GO TO 5026
5022  WRITE(L,5024) II, IHOUR, IDAY
5024  FORMAT(' ',3X,'HP OUTDOOR AT TIME= ',I10,3X,
     1'HOUR= ',I2,3X,'DAY= ',I1)
5026  IF(T(13).EQ.-.1000E-08) GO TO 5032
      GO TO 5036
5032  WRITE(L,5034) II, IHOUR, IDAY
5034  FORMAT(' ',3X,'HP INDOOR AT TIME=',I10,3X,
     1'HOUR= ',I2,3X,'DAY= ',I1)
5036  IF(T(9).EQ.-.1000E-08) GO TO 5042
      GO TO 5046
5042  WRITE(L,5044) II, IHOUR, IDAY
5044  FORMAT(' ',3X,'SAM AT TIME=',I10,3X,
```

```
     1'HOUR= ',I2,3X,'DAY= ',I1)
5046 IF(T(10).EQ.-.1000E-08) GO TO 5052
     GO TO 5056
5052 WRITE(L,5054) II, IHOUR,IDAY
5054 FORMAT(' ',3X,'OFF PEAK AT TIME =',I10,3X,
     1'HOUR= ',I2,3X,'DAY= ',I1)
5056 IF(T(26).EQ.-.1000E-08) GO TO 5062
     GO TO 5066
5062 WRITE(L,5064) II, IHOUR, IDAY
5064 FORMAT(' ',3X,'HEAT,SOLAR TO SPACE AT TIME=',I10,3X,
     1'HOUR= ',I2,3X,'DAY= ',I1)
5066 IF(T(27).EQ.-.1000E-08) GO TO 5072
     GO TO 5076
5072 WRITE(L,5074) II, IHOUR, IDAY
5074 FORMAT(' ',3X,'SOLAR TO STORAGE AT TIME=',I10,3X,
     1'HOUR= ',I2,3X,'DAY= ',I1)
5076 IF(T(28).EQ.-.1000E-08) GO TO 5082
     GO TO 5096
5082 WRITE(L,5084) II, IHOUR, IDAY
5084 FORMAT(' ',3X,'HEAT STORAGE TO SPACE AT TIME=',I10,3X,
     1'HOUR= ',I2,3X,'DAY= ',I1)
5096 IF(T(14).EQ.-.1000E-08) GO TO 5102
     GO TO 5106
5102 WRITE(L,5104) II, IHOUR, IDAY
5104 FORMAT(' ',3X,'INTERIOR LOAD AT TIME= ',I10,3X,
     1'HOUR= ',I2,3X,'DAY= ',I1)
5106 IF(T(25).EQ.-.1000E-08) GO TO 5112
     GO TO 5116
5112 WRITE(L,5114) II, IHOUR, IDAY
5114 FORMAT(' ',3X,'HP TO SPACE AT TIME=',I10,3X,
     1'HOUR= ',I2,3X,'DAY= ',I1)
5116 CONTINUE
C  STOL=TOTAL STORAGE LOSSES (BTU) FOR THE PERIOD
     PBLOSS=6.7996*T(17)+2.4023*(T(18)+T(19)+T(20)+T(21)+
     1T(22))+18.753*T(23)-37.564*T(7)
     STOL=STOL+PBLOSS
C  DL1=DUCT LOSS (BTU) EACH HOUR IN COLLECTOR TO SPACE MODE
     UA=232.0*0.17
C  ADEN=AIR DENSITY (LBM/CU.FT.)
     ADEN=0.07607-0.00017*(T(7)-60.0)+0.000026*(T(7)-T(8))
     TE=(T(26)-T(30)*775.0)*F(26)*3.413/(ADEN*0.245*60.0*
     1520.0)+T(7)
     Y=28.8*520.0*ADEN/UA
     T1=(TE*(Y-1.0)+2.0*T(7))/(Y+1.0)
     DL1=(UA*((TE+T1)/2.0-T(7)))*T(30)
C  DL2=DUCT LOSS (BTU) HOURLY IN COLLECTOR TO STORAGE MODE
     UA=0.17*40.0
     Y=28.8*563.0*ADEN/UA
     TE=(T(17)*(Y+1.0)-2.0*T(7))/(Y-1.0)
     DL2=UA*((T1+T(17))/2.0-T(7))
     UA=45.0
     DL2=DL2+UA*(TE-T(7))
```

```
      UA=0.17*297.0
      TEE=(TE*(Y+1.0)-2.0*T(7))/(Y-1.0)
      DL2=(DL2+UA*((TE+TEE)/2.0-T(7)))*T(31)
      DLC=(232.0*0.17*((TEE+TE)/2.0-T(7)))*T(31)
C   DL3=DUCT LOSS (BTU) HOURLY IN STORAGE TO SPACE MODE
      UA=0.17*40.0
      Y=28.8*1235.0*ADEN/UA
      T1=(T(17)*(Y-1.0)+2.0*T(7))/(Y+1.0)
      DL3=UA*((T1+T(17))/2.0-T(7))
      DL3=DL3+45.0*(T1-T(7))
      UA=40.16
      T11=(T1*(Y-1.0)+2.0*T(7))/(Y+1.0)
      DL3=(DL3+UA*((T11+T1)/2.0-T(7)))*T(32)
C   DL4=DUCT LOSS (BTU) HOURLY IN HEAT PUMP TO SPACE
      TE=T(25)*F(25)*3.4


      UA=20.0*0.17+39.7*0.26
      Y=28.8*980.0*ADEN/UA
      T1=(TE*(Y-1.0)+2.0*T(7))/(Y+1.0)
      DL4=(UA*((TE+T1)/2.0-T(7)))*T(29)
C   DL5=DUCT LOSS (BTU) HOURLY IN OFF-PEAK TO STORAGE
      TIMOP=T(10)/(16600.0+775.0)
      IF(TIMOP.GT.1.0) TIMOP=1.0
      UA=50.0*0.17
      TE=136.0
      Y=28.8*844.0*0.069/UA
      T1=(TE*(Y-1.0)+2.0*T(7))/(Y+1.0)
      DL5=UA*((T1+TE)/2.0-T(7))
      DL5=DL5+45.0*(T1-T(7))
      UA=40.0*0.17
      DL5=(DL5+UA*((T1+T(17))/2.0-T(7)))*TIMOP
C   TOTDL2=TOTAL DUCT LOSS, COLLECTOR-TO-STORAGE
      TOTDL2=TOTDL2+DL2
C   TOTDL5=TOTAL DUCT LOSS OFF-PEAK TO STORAGE
      TOTDL5=TOTDL5+DL5
C   ELECTRIC POWER CONSUMPTIONS NOW FOLLOW:
C   HPAX=HEAT PUMP AUXILIARY ENERGY (BTU) FOR THE PERIOD
      HPAX=HPAX+T(11)*3.413
C   HPIN=HEAT PUMP INDOOR UNIT ENERGY "    "    "     ".
      HPIN=HPIN+T(13)*3.413
C   HPOD=HEAT PUMP OUTDOOR UNIT ENERGY "    "    "     ".
      HPOD=HPOD+T(12)*3.413
C   SAME=SOLAR AIR MOVER ENERGY  "     "    "    "     ".
      SAME=SAME+T(9)*3.413
C   OPT=OFF-PEAK ENERGY   "      "     "    "    "     ".
      OP=T(10)*3.413*16600.0/(16600.0+775.0)
      OPT=OPT+OP
C   EN =TOTAL INTERIOR LOAD (BTU) FOR THE PERIOD
      EN=EN+T(14)*3.413
C   PWR=TOTAL ELECTRICAL ENERGY (BTU) SUPPLIED TO THE
C   BUILDING INCLUDING THE INTERNAL LOADS.
```

```
      PWR=OP+(T(9)+T(11)+T(12)+T(13)+T(14))*3.413
C     HEAT FLOWS NOW FOLLOW:
C     SOLCOL=SOLAR ENERGY (BTU) COLLECTED HOURLY
C     SOLSP=SOLAR ENERGY (BTU) COLLECTED IN SPACE MODE.
C     SOLST=SOLAR ENERGY (BTU) COLLECTED IN STORAGE MODE.
      SOLSP=(T(26)*F(26)-775.0*T(30))*3.413+DL1
      SOLST=(T(27)*F(27)-775.0*T(31))*3.413+DLC
      SOLCOL=SOLSP+SOLST
C     TSOLSP=SOLAR ENERGY (BTU) SENT TO SPACE FOR PERIOD.
      TSOLSP=TSOLSP+SOLSP
C     TSOLST=SOLAR ENERGY (BTU) SENT TO STORAGE FOR PERIOD.
      TSOLST=TSOLST+SOLST-DL2
C     SOLCOT=SOLAR ENERGY (BTU) COLLECTED FOR THE PERIOD.
      SOLCOT=SOLCOT+SOLCOL
C     QCOP=HEAT PUMP PERFORMANCE
      IF(T(29).LT.0.98) GO TO 505
      QCOP=(T(25)*F(25)*3.413+DL4)
      1/(T(13)*3.413+T(12)*3.413)
      TEMPF=1.8*T(2)+32.0
      WRITE(L,507) QCOP, TEMPF, II
507   FORMAT(' ',3X,'HEAT PUMP COP=',F6.3,3X,'OUTDOOR DBT=',
      1F4.1,' DEG F.',3X,'HOUR=',I5)
C     HPSP=ENERGY (BTU) DELIVERED TO SPACE VIA HEAT PUMP.
505   HPSP=HPSP+T(25)*F(25)*3.413+DL4
C     OPST=OFF-PEAK TO STORAGE
      OPST=OPST+OP-DL5
C     SAM HEAT CONTRIBUTIONS (BTU) FOR THE PERIOD FOLLOW:
      SOP=SOP+T(10)*3.413*775.0/(16600.0+775.0)
      SSTSP=SSTSP+775.0*3.413*T(32)
      SSCSP=SSCSP+775.0*3.413*T(30)
      SSCST=SSCST+775.0*3.413*T(31)
C     A***** ARE ACTUAL SAM CONTRIBUTIONS NORMALIZED TO SAME:
      ASOP=SOP*SAME/(SOP+SSTSP+SSCSP+SSCST)
      ASSTSP=SSTSP*SAME/(SOP+SSTSP+SSCSP+SSCST)
      ASSCSP=SSCSP*SAME/(SOP+SSTSP+SSCSP+SSCST)
      ASSCST=SSCST*SAME/(SOP+SSTSP+SSCSP+SSCST)
C     STSP=ENERGY (BTU) FROM STORAGE TO SPACE FOR PERIOD.
      STSP=STSP+(T(28)*F(28)-775.0*T(32))*3.413+DL3
C     CALCULATION OF MAXIMUM COLLECTOR EFFICIENCY DURING ANY
C     ONE HOUR.  TIM=HOUR OF MAXIMUM EFFICIENCY.
      IF(SUN.LE.2.0E+04) GO TO 650
      CE=SOLCOL/SUN
      IF(CE.GT.CEMAX) GO TO 600
      GO TO 650
600   CEMAX=CE
      TIM=FLOAT(II)


      JHOUR=IHOUR
650   CONTINUE
      IF(IDAY.GT.5) GO TO 900
      IF(IHOUR.GT.6.AND.IHOUR.LT.14) GO TO 800
```

```
      IF(IHOUR.GT.18.AND.IHOUR.LT.23) GO TO 800
      GO TO 900
800   ONPK=ONPK+PWR
      GO TO 950
900   OFFPK=OFFPK+PWR
950   CONTINUE
      IHOUR=IHOUR+1
      IF(IHOUR.LT.24) GO TO 1000
      IHOUR=0
      IDAY=IDAY+1
      IF(IDAY.GT.7) IDAY=1
1000  READ(40,255,END=1025) II,(T(I),I=2,8)
C  COLLECTION EFFICIENCY FOR THE PERIOD:
1025  COLEF=SOLCOT/TSUN
C  CALCULATION FOR SOLAR COP NOW FOLLOWS:
      SOLCOP=(SOLCOT+ASSCSP+ASSCST+ASSTSP*TSOLST/(TSOLST+OPST))
      1/(ASSCSP+ASSCST+ASSTSP*TSOLST/(TSOLST+OPST))
C  CALCULATION OF SYSTEM COP=TOTAL HEAT DELIVERED TO
C  SYSTEM / TOTAL ENERGY THAT COSTS.
      SYSCOP=(SAME+OPT+EN+SOLCOT+HPSP)/
      1(ONPK+OFFPK)
C  HPCOP=HEAT PUMP COP
      HPCOP=HPSP/(HPAX+HPIN+HPOD)
      HPCOPW=HPSP/(HPIN+HPOD)
C  THE FOLLOWING CONVERTS ALL QUANTITIES TO KBTU:
      HPIN=HPIN/1000.0
      HPOD=HPOD/1000.0
      HPAX=HPAX/1000.0
      SAME=SAME/1000.0
      EN=EN/1000.0
      OPT=OPT/1000.0
      ONPK=ONPK/1000.0
      OFFPK=OFFPK/1000.0
      TSUN=TSUN/1000.0
      TSOLSP=TSOLSP/1000.0
      SOLCOT=SOLCOT/1000.0
      TSOLST=TSOLST/1000.0
      STSP=STSP/1000.0
      ASSTSP=ASSTSP/1000.0
      ASSCSP=ASSCSP/1000.0
      ASSCST=ASSCST/1000.0
      ASOP=ASOP/1000.0
      TOTDL2=TOTDL2/1000.0
      TOTDL5=TOTDL5/1000


      STOL=STOL/1000.0
      HPSP=HPSP/1000.0
      OPST=OPST/1000.0
      QTOSPA=TSOLSP+STSP+ASSTSP+ASSCSP+TOTDL2+TOTDL5+
      1STOL+HPSP
      QTOSTO=TSOLST+ASSCST+ASOP+OPST
```

```
      QFRSTO=STSP+STOL
      WRITE(L,1050)
1050  FORMAT('1',44X,'SOLAR-AUGMENTED HEAT PUMP SYSTEM')
      WRITE(L,1060) ISTART,ISTOP
1060  FORMAT(' ',40X,'BEGINNING AT ',I5,' AND ENDING AT ',
     1I5,' HOURS.')
      WRITE(L,1070)
1070  FORMAT('-',35X,'ELECTRICAL ENERGY DISTRIBUTION',
     17X,'(KBTU):')
      WRITE(L,1080) HPIN
1080  FORMAT('0',39X,'HEAT PUMP INDOOR UNIT          ',F12.2)
      WRITE(L,1090) HPOD
1090  FORMAT(' ',39X,'HEAT PUMP OUTDOOR UNIT         ',F12.2)
      WRITE(L,1100) HPAX
1100  FORMAT(' ',39X,'HEAT PUMP AUXILIARY            ',F12.2)
      WRITE(L,1110) SAME
1110  FORMAT(' ',39X,'SOLAR AIR MOVER                ',F12.2)
      WRITE(L,1112) EN
1112  FORMAT(' ',39X,'TOTAL INTERIOR LOAD            ',F12.2)
      WRITE(L,1115) OPT
1115  FORMAT(' ',39X,'OFFPEAK HEATER                 ',F12.2)
      WRITE(L,1120) ONPK
1120  FORMAT(' ',39X,'TOTAL USED ONPEAK              ',F12.2)
      WRITE(L,1130) OFFPK
1130  FORMAT(' ',39X,'TOTAL USED OFFPEAK             ',F12.2)
      WRITE(L,1140)
1140  FORMAT('-',35X,'THERMAL ENERGY FLOWS',17X,
     1'(KBTU):')
      WRITE(L,1150) TSUN
1150  FORMAT('0',39X,'INSOLATION FOR PERIOD          ',F12.2)
      WRITE(L,1155) SOLCOT
1155  FORMAT(' ',39X,'TOTAL SOLAR COLLECTED          ',F12.2)
      WRITE(L,1160) TSOLSP
1160  FORMAT(' ',39X,'SOLAR TO SPACE                 ',F12.2)
      WRITE(L,1170) TSOLST
1170  FORMAT(' ',39X,'SOLAR TO STORAGE               ',F12.2)
      WRITE(L,1180) STSP
1180  FORMAT(' ',39X,'STORAGE TO SPACE               ',F12.2)
      WRITE(L,1190) ASSTSP
1190  FORMAT(' ',39X,'SAM, STORAGE TO SPACE          ',F12.2)
      WRITE(L,1200) ASSCSP
1200  FORMAT(' ',39X,'SAM, COLLECTOR TO SPACE        ',F12.2)
      WRITE(L,1210) ASSCST
1210  FORMAT(' ',39X,'SAM, COLLECTOR TO STORAGE      ',F12.2)
      WRITE(L,1220) ASOP
1220  FORMAT(' ',39X,'SAM, OFFPEAK TO STORAGE        ',F12.2)
      WRITE(L,1230) TOTDL2
1230  FORMAT(' ',39X,'DUCT LOSSES (COLL->STORAGE)    ',F12.2)
      WRITE(L,1235) TOTDL5
1235  FORMAT(' ',39X,'DUCT LOSSES (OFFPEAK->STORAGE)',F11.2)
      WRITE(L,1240) STOL
1240  FORMAT(' ',39X,'STORAGE LOSSES TO SPACE        ',F12.2)
```

```
      WRITE(L,1250) HPSP
1250  FORMAT(' ',39X,'HEAT PUMP TO SPACE          ',F12.2)
      WRITE(L,1260) OPST
1260  FORMAT(' ',39X,'OFFPEAK TO STORAGE          ',F12.2)
      WRITE(L,1270) QTOSPA
1270  FORMAT('0',39X,'TOTAL HEAT TO SPACE         ',F12.2)
      WRITE(L,1280) QTOSTO
1280  FORMAT(' ',39X,'TOTAL HEAT TO STORAGE       ',F12.2)
      WRITE(L,1290) QFRSTO
1290  FORMAT(' ',39X,'TOTAL HEAT FROM STORAGE     ',F12.2)
      WRITE(L,1300)
1300  FORMAT('-',35X,'SYSTEM PERFORMANCE:')
      WRITE(L,1310) CEMAX, TIM, JHOUR
1310  FORMAT('0',30X,'MAXIMUM COLLECTION EFFICIENCY FOR
     1 ONE HOUR =',F6.3,' FOUND AT TIME = ',F6.1,
     12X,'HOUR= ',I2)
      WRITE(L,1320) COLEF
1320  FORMAT(' ',30X,'COLLECTION EFFICIENCY =',F6.3)
      WRITE(L,1350) HPCOPW
1350  FORMAT(' ',30X,'HEAT PUMP COP = ',F6.3)
      WRITE(L,1355) HPCOP
1355  FORMAT(' ',30X,'HEAT PUMP COP INCLUDING AUX HTR=',F6.3)
      WRITE(L,1360) SYSCOP
1360  FORMAT(' ',30X,'SYSTEM COP = ',F6.3)
      WRITE(L,1370) SOLCOP
1370  FORMAT(' ',30X,'SOLAR COP = ',F6.3)
      CLOSE(UNIT=40,DIRECTORY='22665,212266')
      STOP
      END
```

Sample Report

SOLAR-AUGMENTED HEAT PUMP SYSTEM
BEGINNING AT 7896 AND ENDING AT 8064 HOURS.

ELECTRICAL ENERGY DISTRIBUTION	(KBTU):
HEAT PUMP INDOOR UNIT	42.03
HEAT PUMP OUTDOOR UNIT	295.26
HEAT PUMP AUXILIARY	89.51
SOLAR AIR MOVER	246.72
TOTAL INTERIOR LOAD	700.60
OFFPEAK HEATER	711.23
TOTAL USED ONPEAK	483.80
TOTAL USED OFFPEAK	1601.55

THERMAL ENERGY FLOWS	(KBTU):
INSOLATION FOR PERIOD	3000.39
TOTAL SOLAR COLLECTED	1299.67
SOLAR TO SPACE	277.68
SOLAR TO STORAGE	945.23
STORAGE TO SPACE	1594.88
SAM, STORAGE TO SPACE	114.32
SAM, COLLECTOR TO SPACE	16.31
SAM, COLLECTOR TO STORAGE	69.28
SAM, OFFPEAK TO STORAGE	46.80
DUCT LOSSES (COLL->STORAGE)	76.77
DUCT LOSSES (OFFPEAK->STORAGE)	49.34
STORAGE LOSSES TO SPACE	96.63
HEAT PUMP TO SPACE	752.86
OFFPEAK TO STORAGE	661.89
TOTAL HEAT TO SPACE	2978.79
TOTAL HEAT TO STORAGE	1723.20
TOTAL HEAT FROM STORAGE	1691.51

SYSTEM PERFORMANCE:

COLLECTION EFFICIENCY = 0.433
HEAT PUMP COP = 1.764
SYSTEM COP = 1.816
SOLAR COP = 9.504

VITA

John J. Tomlinson was born in Gulfport, Mississippi on October 1, 1944. He attended elementary and secondary schools in Laurel, Mississippi and graduated from George S. Gardiner high school in 1962. He entered the University of Mississippi for two years of undergraduate study in Electrical Engineering. He continued his education at Mississippi State University where he received both a Bachelor of Science in Physics in 1967 and a Master of Science in Physics in 1969.

After teaching in the Science Department at Jones County Junior College in Ellisville, Mississippi for nine years, he entered the Graduate School of the University of Tennessee, Knoxville in September 1978, and received a Master of Science degree in Mechanical Engineering in August 1980.

The author is a member of the American Society of Mechanical Engineers and the International Solar Energy Society. He will be employed in the Engineering Technology Division of Oak Ridge National Laboratory after graduation.